The role of ASK1 in selective striatal lesion formation induced by neuronal injury

Kyoung Joo Cho

Department of Medical Science

The Graduate School, Yonsei University

The role of ASK1 in selective striatal lesion formation induced by neuronal injury

Directed by Professor Jong Eun Lee

The Doctoral Dissertation
submitted to the Department of Medical Science,
the Graduate School of Yonsei University
in partial fulfillment of the requirements for the degree
of Doctor of Philosophy

Kyoung Joo Cho

December 2014

This certifies that the Doctoral Dissertation of Kyoung Joo Cho is approved.

Thesis Supervisor : Jong Eun Lee

Thesis Committee Member#1 : Won Taek Lee

Thesis Committee Member#2 : Kyung Ah Park

Thesis Committee Member#3 : Se Hoon Kim

Thesis Committee Member#4 : Chul Hoon Kim

The Graduate School
Yonsei University

December 2014

ACKNOWLEDGEMENTS

TABLE OF CONTENTS

PART II

Apoptosis signal-regulating kinase-1 aggravates ROS-mediated striatal degeneration in 3-nitropropionic acid-infused mice

PART III

Apoptosis signal-regulating kinase 1 mediates 3-nitropropionic acid toxicity and regulates C1q level via astrocyte TGF-beta

LIST OF FIGURES

PART I

Inhibition of ASK1 reduces ER stress and nuclear huntingtin fragments in a mouse model of Huntington Disease

PART II

Apoptosis signal-regulating kinase-1 aggravates ROS-mediated striatal degeneration in 3-nitropropionic acid-infused mice

PART III

Apoptosis signal-regulating kinase 1 mediates 3-nitropropionic acid toxicity and regulates C1q level via astrocyte TGF- β1

<ABSTRACT>

The role of ASK1 in selective striatal lesion formation induced by neuronal injury

Kyoung Joo Cho

Department of Medical Science
The Graduate School, Yonsei University

(Directed by Professor Jong Eun Lee)

Apoptosis signal-regulating kinase-1 (ASK1), an early signaling element in the cell death pathway, has been suggested to participate in the pathology of neurodegenerative diseases, which may be associated with environmental factors that impact the diseases. The systemic administration of 3-nitropropionic acid (3-NP) facilitates the development of selected striatal lesions and it remains unclear whether specific neurons are selectively targeted in 3-NP infused striatal degeneration. Although not entirely elucidated, the mechanisms of neurotoxicity induced by 3-NP have been shown to include the exhaustion of adenosine triphosphate, mitochondrial membrane depolarization, dysregulation of intracellular calcium homeostasis, calpain activation, and the release of pro-apoptotic proteins from mitochondria. The present study is to characterize the regulation of BDNF in each cortical and striatal subregion. This study investigates that mild and chronic exposure of mitochondrial toxin can modulate the C1q level both in cortex and striatum via regulation of TGF-beta

from astrocyte. Consequently we investigate how the BDNF is dominantly depleted in striatum, and eventually whether striatal lesion is established in involving in ASK1 pathway.

The results of the present work show an alteration of ASK1 pathway molecules, TGF-beta, C1q level, and BDNF level as a final standard to striatal degeneration. By ASK1 down-regulation, improvement in each molecules containing behavioral impairment was evaluated in 3NP- infused mice and 3-NP treated primary neuronal cells. We propose the hypothesis that (1) ASK1 overexpression by systemic infusion of 3-NP promotes the formation of selective striatal lesions, and this occurs apart from just ROS generation. (2) ASK1 may differentially regulate C1q secretion level via active TGF-beta in each brain subregion of cortex and striatum, consequently involved in axon degeneration of corticostriatal projection neuron. When brain is mildly and chronically exposed to mitochondrial toxin, presynaptic neuron (in cortical neuron) degrades first, and then postsynaptic neuron of striatal MSN neuron withers as a consequence of it.

Consolidating these results, we suggest that the increased ASK1 is linked to regulation of TGF-beta secreted in astrocytes, and differential C1q expression in neurons triggered by TGF-beta leads degradation of cortical projection and depletion of BDNF in striatal neuron in mice brains systemically infused with 3-NP.

Key words : apoptosis signal-regulating kinase 1, 3-nitropropionic acid, Huntington's disease, brain derived neurotrophic factor, siRNA, superoxide dismutase

PART I

Inhibition of ASK1 reduces ER stress and nuclear huntingtin fragments in a mouse model of Huntington Disease

I. INTRODUCTION

Accumulation of misfolded proteins within the endoplasmic reticulum (ER) lumen induces ER stress, which has been implicated in human diseases such as Alzheimer's disease [1], Parkinson's disease [2], and Huntington's disease (HD) [3]. HD is characterized clinically by chorea, psychiatric disturbances, and dementia, while it is characterized pathologically by neuronal inclusions as well as striatal and cortical neurodegeneration. The neurodegeneration is arisen from the loss of long projection neurons in the cortex and striatum [4]. HD is inherited in an autosomal dominant manner, and is caused by the presence of an elongated polyglutamine (polyQ) tract (> 40) in the huntingtin (htt) gene [5].

Htt fragments with pathogenic repeat lengths have been reported to co-localize with various molecular chaperones [6,7] and proteasome components and to impair the function of the ubiquitin-proteasome system (UPS) [8], resulting in ER stress [9]. Apoptosis signal-regulating kinase 1 (Ask1) is reported to be involved in ER stress triggered by htt fragments, which results in neuronal cell death. ER stress activates Ask1 through the formation of the IRE1-TRAF2-Ask1 complex. Furthermore, the expanded polyQ portion of htt activates Ask1, and it has been shown conclusively that Ask1 is required for polyQ-induced neuronal cell death [3,4,10,11]. Nevertheless, despite the numerous *in vitro* studies supporting a correlation between Ask1 and ER stress, it is not known whether the level of ER stress and Ask1 protein levels or activity are increased *in vivo* in HD transgenic (tg) animals. In HD, Ask1 is thought to be a modifier of htt at the gene level [12], a signal transducer at the protein level [10], and a cell death modulator at the post-translational level [13]. It has also been suggested that the manifestation, progression, and outcome of HD may be affected by modifier genes and environmental factors that impact the disease's

presentation [12].

In this study, we investigated the role of Ask1 in the pathogenesis of HD transgenic (tg) mice. Specifically, we analyzed the expression of Ask1 and htt within the striatum and cortex along with ER stress in each region, and determined whether Ask1 interacts with htt fragments *in vivo*. Additionally, we assessed the levels of brain-derived neurotrophic factor (BDNF) in a region-specific manner, and examined the effects of inactivation of Ask1 on striatal atrophy and motor dysfunction.

II. MATERIALS AND METHODS

1. Animal model

In this study, 8-week and 12-week R6/2 HD male tg (The Jackson Laboratory, Bar Harbor, ME, U.S.A.), littermate wt mice were used. All procedures were performed in accordance with the guidelines for the care and use of laboratory animals (Yonsei University, Seoul, Korea), which are approved by the Association for Assessment and Accreditation of Laboratory Animal Care (AAALAC). Animals were anesthetized with 2.0% isoflurane under 30% oxygen and 70% nitrous oxide using a vaporizer (VMC Anesthesia Machine, MDS matrix, Orchard Park, NY, U.S.A.). Rectal temperature was controlled at 37±0.5℃ with a homeothermic blanket.

2. Immunohistochemistry

To determine the pattern of localization of htt (Epitomics, Burlingame, CA, U.S.A; 1C2, Chemicon, Bedford, MA, U.S.A.) and Ask1 (Santa Cruz Biotechnology, Santa Cruz, CA, U.S.A.), we performed immunofluorescent staining. After sacrificing the animals, their brains were removed, postfixed o vernight in 3.7% formaldehyde, and stored in 30% sucrose. After fixation, the brains were cut into coronal sections of 20 μm thickness on a cryostat section and processed for immunohistochemistry. Fixed sections were incubated with the blocking solution as described previously [14] and incubated with a prim ary antibody, rabbit polyclonal anti-htt antibody (1:100, Epitomics). After washing, the sections were incubated with FITC-conjugated donkey anti-rabbit IgG (1:200, Jackson ImmunoResearch, West Grove, PA, USA). For counter-staining, the sections were incubated with propidum iodine (PI, 1:5000, Sigma, St. Louis, MO, U.S.A.). The stained tissue samples were washed and

mounted using Vectashield mounting medium (Vector Lab, Burlingame, CA, U.S.A.). These sections were observed under a LSM510 confocal laser scanning microscope (Carl Zeiss, Thornwood, NY, U.S.A.).

For immunofluorescent double-labeling with htt and Ask1, htt (1:100, Epitomics) immunohistochemistry was performed as described above, followed by incubation with Cy™ 3-conjugated donkey anti-rabbit IgG (1:200, Jackson ImmunoResearch). After washing, the sections were incubated with the blocking solution and reacted with goat anti-Ask1 antibody (1:100, Santa Cruz Biotechnology), followed by FITC-conjugated donkey anti-goat IgG (1:200, Jackson ImmunoResearch). The sections were then covered with a cover-slip and examined under a confocal microscope (Carl Zeiss).

3. Western blot analysis and co-immunoprecipitation

The expression levels of proteins were analyzed by western blotting. The cortex or striatum of dissected animal brains were lysed in lysis buffer (20 mM Hepes–KOH, pH 7.5, 250 mM sucrose, 10 mM KCl, 1.5 mM $MgCl_2$, 1 mM EDTA, 1 mM EGTA, 0.5 mM PMSF, 0.1 mM sodium vanadate, and 0.1 mM proteinase inhibitor cocktail). The samples were homogenized by douncing with a Teflon homogenizer (Wheaton, Millville, NJ, U.S.A.) and centrifuged at 8,000 *g* for 20 min at 4℃. The lysates were loaded onto SDS-polyacrylamide gels. After migration, the proteins were electrotransfered onto a polyvinylidine difluoride membrane (PVDF) (Millipore, Bedford, MA, U.S.A), which was blocked in 5% skim milk, incubated with primary antibodies; Ask1 (1:1000, Cell Signaling, Danvers, MA, U.S.A.), pAsk1 (1:1000, Cell Signaling), 1C2 (1:5000, Chemicon, Bedford, MA, U.S.A.), htt (1:1000, Epitomics), or BDNF (1:500, Abchem, Cambridge, UK). After washing, blots were incubated with HRP-conjugated secondary antibodies (1:5000, Roche Diagnostics, Indianapolis,

IN, U.S.A.) and the bands were visualized with an enhanced chemiluminescence reagent (Amersham Biosciences, Piscataway, NJ, U.S.A.). To separate the cytosolic and nuclear fractions of the proteins, each sample was homogenized briefly in lysis buffer and then spun down at 750 *g* for 10 minutes at 4℃. The pellet containing the nuclear fraction was resuspended with lysis buffer. The resuspened solution was centrifuged at 16,000 *g* for 20 min at 4℃and the supernatant was used as the nuclear fraction. The supernatant obtained after centrifugation at 750 g for 10 minutes was then centrifuged at 10,000 *g* for 20 min at 4℃, and the supernatant containing the cytosolic fraction was transferred to a new tube. This tube was centrifuged at 100,000 *g* for 1 hr at 4℃ and the supernatant obtained was designated the cytosol.

The procedure for co-immunoprecipitation was performed as described previously with some modifications [15]. The cortex and striatum were removed from mice brains, and prepared in the same manner as for western blotting. The protein samples were incubated in a 50% slurry of protein A-sepharose (Amersham Biosciences), and this mixed sample was centrifuged at 12,000 *g* for 1 min at 4℃. The supernatant was incubated with 20 μl of protein A-sepharose for 2 hr at 4℃ and then incubated with 2 μg of goat anti-Ask1 antibody (1:1000; Santa Cruz Biotechnology) overnight at 4℃. The pellets were washed by centrifugation at 14,000 *g* for 3 min at 4℃. After centrifugation, the supernatant was immunoblotted with polyclonal rabbit anti-htt antibody (1:1000; Epitomics) and with mouse anti-Ask1 antibody as a control.

4. RT-PCR Analysis

Total RNA was isolated from the striatum and cortex of the mice. Total RNA (1 μg) was reverse-transcribed and cDNA was synthesized using PCR. The primers used are shown in Table 1. PCR was performed as follows: initial

denaturation at 95℃ for 10 min, amplification (30 cycles) for 30 sec at 95℃, 30 sec at 60℃, and 30 sec at 72℃, and a final extension at 70℃ for 10 min. To semi-quantify BDNF mRNA levels without performing real-time PCR, we performed the PCR reaction for different numbers of cycles (15, 20, 25, and 30 cycles). RT-PCR products were visualized with a UV illuminator after electrophoresis on an agarose gel.

5. Neutralization of Ask1 using an anti-Ask1-antibody

To inactivate Ask1 for an extended period of time (several weeks), we used an Ask1 antibody raised against an epitope corresponding to amino acids at the C-terminus of the Ask1 protein. The antibody was added to the dried BioPORTER (Quiktease protein delivery kit, Sigma Aldrich) reagent and allowed to incubate at room temperature for 10 min according to the manufacturer's protocol [16]. The mixture of Ask1 antibody and BioPORTER was loaded into an osmotic reservoir. Mice were anesthetized as described above and placed in a stereotaxic apparatus. A micro-osmotic pump reservoir (Alzet, Cupertino, CA, U.S.A.) containing anti-Ask1 antibody (0.2 mg/ml in saline, Santa Cruz) was placed subcutaneously on the backs of the animals [17]. A brain infusion cannula connected to the pump was positioned at the intra-striatum (anterial, 0.7 mm; lateral, 1.2 mm; and depth, -3.3 mm). As a control, rabbit IgG or pre-immune Ask1 antibody was infused in the same way. The infusion rate was 1.0 μl/h and the pump infused the designated solution for 4 weeks into the brains of HD tg mice. After implantation of the osmotic pump at the age of 8-weeks, the mice were sacrificed 4 weeks later [18].

6. Rotarod test

The motor function of model animals was assessed with a rotarod

apparatus (Ugo Basile North America Inc., Schwenksville, PA, U.S.A.), where the time a mouse was able to remain on the rod was measured at an accelerating speed from 4 to 40 rpm [19]. Each mouse was trained for 5 min and the training session was followed by a 30 min rest period. Mice were then placed back on the rotarod for five trials of a maximum of 5 min at accelerating speed. Mice were evaluated for 3 consecutive days.

7. Striatal lesion analysis

Four weeks after Ask1 inhibition with antibody, animals were anesthetized and decapitated. Brains were frozen and cut on a cryostat into 20 μm sections from the anterior to the posterior at 500 μm intervals. The sections were stained with cresyl violet and then scanned with an LAS1000 imaging densitometer (Fujifilm, Tokyo, Japan). Striatal atrophy was identified as a striatal region size with pallor or loss of cresyl violet staining. The area of the striata was measured using Sigmascan Pro (ver 6.0).

8. Statistical analysis

Data are expressed as mean ± SD. The significance of differences among multiple groups was evaluated by ANOVA followed by Fisher's *post hoc* protected least-significant difference test, while two groups were compared using unpaired *t* tests (StatView, version 5.01; SAS Institute Inc, Cary, NC).

III. RESULTS

1. Levels of ASK1 protein and ER stress are increased in HD mice

In vitro studies in neuronal cell cultures have shown that Ask1 is involved in the pathogenesis of HD [3]. In our western blot assay (Figure 1; n = 6 each), the amount of Ask1 protein was increased in HD mice compared to wt mice; furthermore, higher levels of Ask1 were detected in the cortex than in the striatum of both HD tg and wt mice. Ask1 protein in the cortex was mostly present in the nuclear fraction, and barely detectable in the cytosol; similarly, in the striatum, more Ask1 protein was present in the nuclear fraction than the cytosolic fraction (Figure 1; n = 5).

ER stress was evaluated by assessing the level of CHOP expression using RT-PCR (Figure 2; n = 5 each). Levels of CHOP, a member of the C/EBP family of bZIP transcription factors and an indicator of ER stress, were higher in HD than wt mice. Specifically, CHOP expression was higher in the cortex than in the striatum, which correlates with protein expression level of Ask1.

We confirmed the pattern and cellular localization of fragmented htt in HD mice by immunohistochemistry (Figure 2; n = 5 each). High-magnification imaging of htt immunoreactive neurons in the cortex and striatum revealed a perinuclear pattern of fragmented htt staining. The striatal neurons of HD mice stained relatively weakly for htt, which may reflect the lower level of htt expression in the striatum compared with cortical neurons. When we double-stained for both Ask1 and htt, we found that Ask1 and htt fragments colocalized in the cytsol in both the cortex and striatum (Figure 2; n = 3 each).

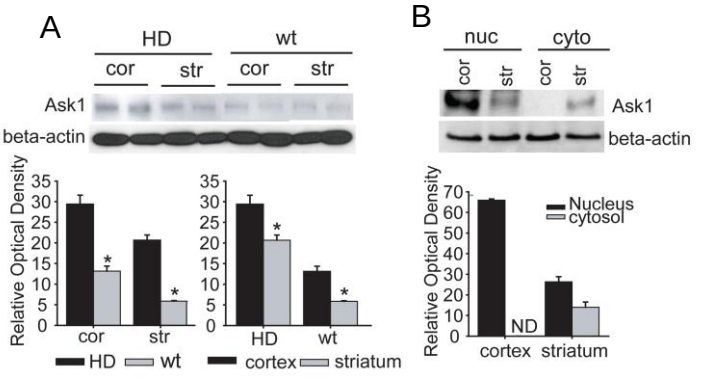

Figure 1. Expression of Ask1 in HD transgenic mice (tg) and HD littermates (wt). (A) Western blot analysis of Ask1 protein in HD and wt mice demonstrates that the Ask1 protein is expressed in cortical and striatal regions, respectively. **(B)** Ask1 protein is expressed at higher levels in the nuclear than in the cytosolic fraction; this is especially noticeable in the cortex.

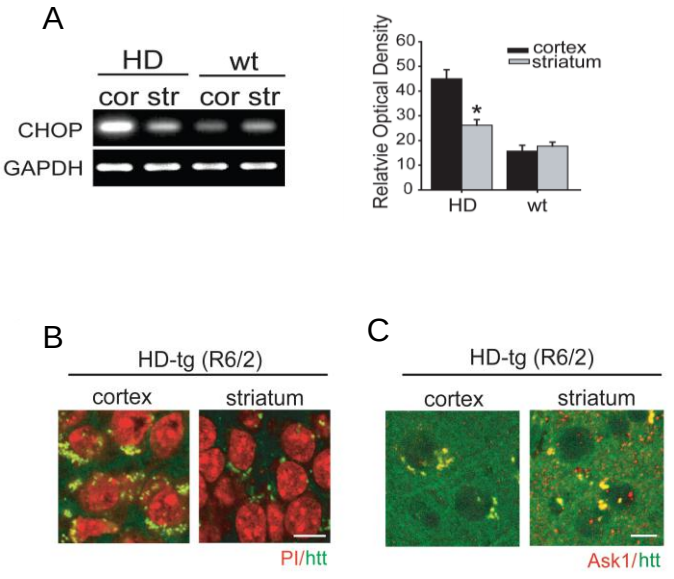

Figure 2. ER stress and expression pattern of Ask1 in HD transgenic mice (tg) and HD littermates (wt). (A) CHOP mRNA expression, a marker of ER stress, was evaluated in the cortex and striatum of HD and wt mice using RT-PCR. CHOP mRNA was highly expressed in the cortex of HD mice. **(B)** immunohistochemical staining of htt. Htt-positive cells show a perinuclear staining pattern in the cytosol of both the cortex and striatum of HD mice. **(C)** Double immunohistochemistry of Ask1 and htt fragments demonstrates that the two molecules are co-localized.

Scale bar = 10 μm; cor, cortex; str, striatum; *$p < 0.01$

2. ASK1 interacts with htt fragments and aids in the translocation of htt

We inhibited Ask1 activity for 4 weeks using an anti-Ask1 antibody, and confirmed that HD mice brains exhibited diminished Ask1 activity under these conditions (Figure 3A; n = 5 each). Infusion of the Ask1 antibody into the striatum of HD mice resulted in a reduction of CHOP expression in both of cortex and striatum (Figure 3B; n = 5 each).

Co-immunoprecipitation and double-immunohistochemistry experiments revealed that inactivated Ask1 bound to htt fragments, and this occurred to a greater extent in the cortex than in the striatum (Figure 4; n = 4 each). The complex of two molecules was mostly shown in the cortex moreover the combined complex was detected in the cytosol than in the nucleus of the cortex. (Figure 4; n = 3 each). Double immunohistochemistry of Ask1 and htt confirmed that inactivated Ask1 and htt fragments co-localized in the cytosol of cortical neurons (Figure 4; n = 4).

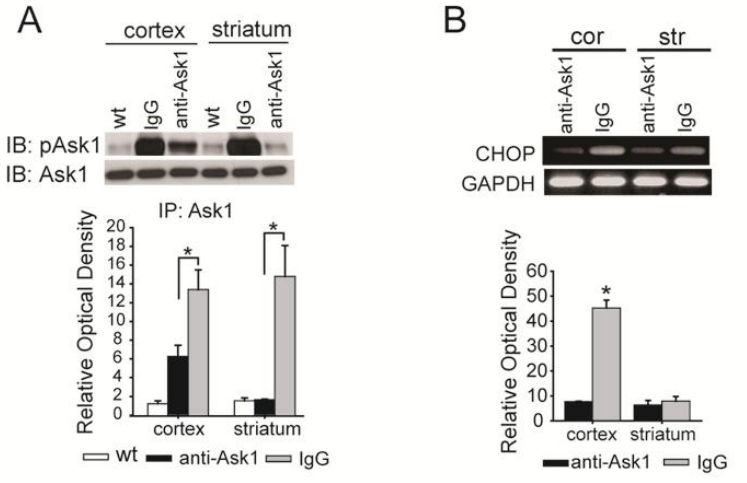

Figure 3. The effect of inhibition of Ask1 on the levels of ER stress and htt fragments in HD. (A) Co-immunoprecipitation of Ask1 and pAsk1 (Thr 845) determined whether Ask1 was inhibited effectively in Ask1 antibody-treated mice. The amount of pAsk1 is significantly reduced in Ask1 antibody-treated HD mice. **(B)** RT-PCR results for CHOP show that ER stress is decreased in both the cortex and striatum of Ask1 antibody-treated HD mice. *$p < 0.01$

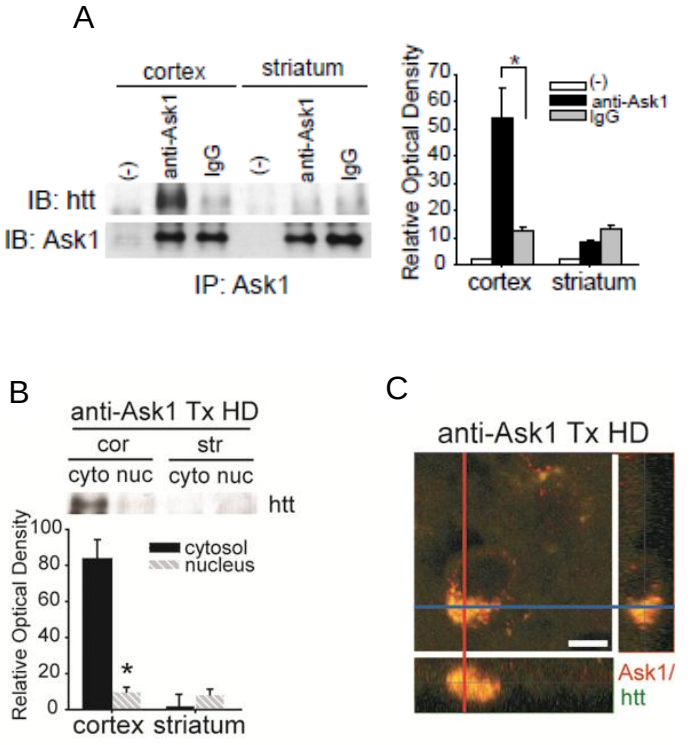

Figure 4. The effect of neurtralizing Ask1 on htt fragments localiziation in HD. (A) Inactivated Ask1 interacts with htt fragments. Co-immunoprecipitation of Ask1 and htt fragments in the cortex and striatum of Ask1 antibody-treated HD and IgG/preimmune antibody-treated HD mice. **(B)** Co-immunoprecipitation of Ask1 and htt fragments was performed in the subcellular fraction in the both of cortex and striatum. More htt immunoreactive products are present in the cytosol fraction than in the nuclear fraction of the cortex in Ask1 antibody-treated HD mice. **(C)** Cells double positive for Ask1 and htt are detected in the cytosol of the cortical region of Ask1 antibody-treated HD mice.

Scale bar = 5 μm. (-), without antibody; cor, cortex; str, striatum; *$p < 0.01$

3. Inhibition of ASK1 facilitates BDNF transport to the striatum and improves motor dysfunction

BDNF mRNA levels were shown to differ between different brain regions of HD mice, including the cortex and striatum (Figure 5; n = 5 each). There were more BDNF transcripts present in the cortex than in the striatum of wt mice, whereas BDNF mRNA levels in the cortex of HD mice were significantly reduced compared to the level of striatal BDNF mRNA in wt mice. Western blotting of BDNF revealed that inhibition of Ask1 significantly prohibit the reduction of BDNF protein levels in the striatum of HD mice (Figure 5; n = 7 each). Although levels of BDNF protein increased as a result of Ask1 inhibition, there were no significant changes in BDNF mRNA levels between Ask1-inhibited HD (anti-Ask1 treated HD, A) and vehicle-treated HD mice (rabbit IgG treated HD, I) (Figure 5; n = 5 each). Thus, the increase in BDNF protein as a result of the inhibition of Ask1 was not due to an increase in the amount of BDNF transcript.

We next evaluated motor function in HD mice at 12 weeks of age, at which stage brain Ask1 had been inhibited for 4 weeks. There was significant performance impairment in HD mice at 12 weeks of age, indicated by the reduced times these mice were able to stay on the rotarod compared to wt mice (Figure 6; n = 4 each). HD mice treated with Ask1 antibody, however, showed improved motor performance compared to preimmune antibody-treated HD mice. We also assessed the changes in striatal atrophy in Ask1 antibody-treated HD mice by measuring the size of the striatal region (Figure 6, n = 3 each). The striatum was larger in the Ask1 antibody-treated HD mice than naïve HD mice or preimmune antibody-treated HD mice ($p = 0.014$).

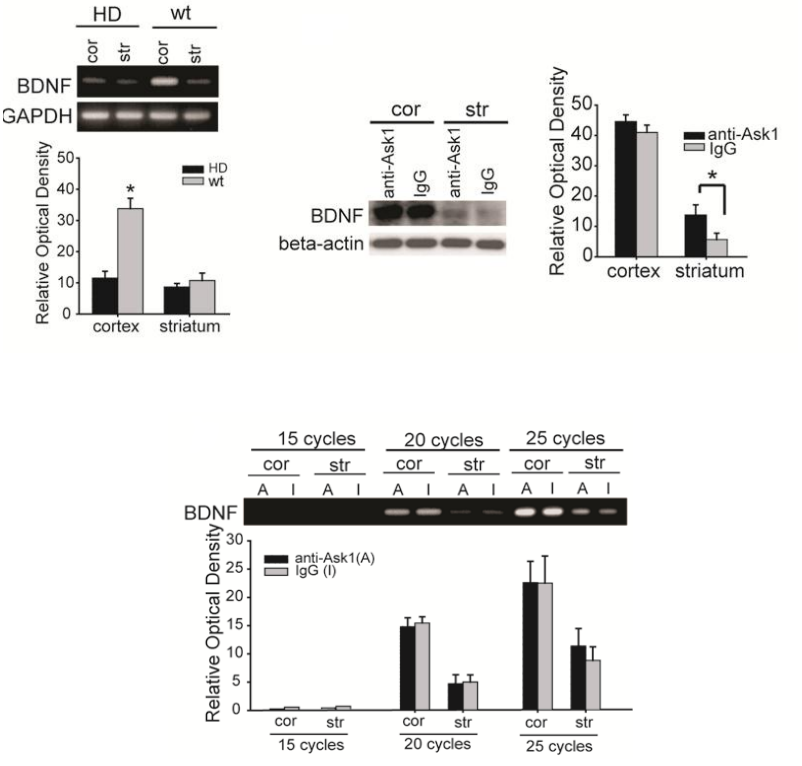

Figure 5. The effect of inhibition of Ask1 on expression of BDNF. BDNF mRNA expression was reduced in both the cortex and striatum of HD mice, whereas BDNF mRNA is expressed at a high level in the cortex of wt mice. Western blot analysis of BDNF protein demonstrates that the level of BDNF expression in the HD mice treated with Ask1 antibody (anti-Ask1) or IgG/preimmune antibody (IgG) increased in the striatum of Ask1 antibody-treated HD mice; BDNF mRNA levels are not significantly different between Ask1 antibody-treated HD (anti-Ask1, A) and IgG/preimmune antibody-treated HD mice (IgG, I)

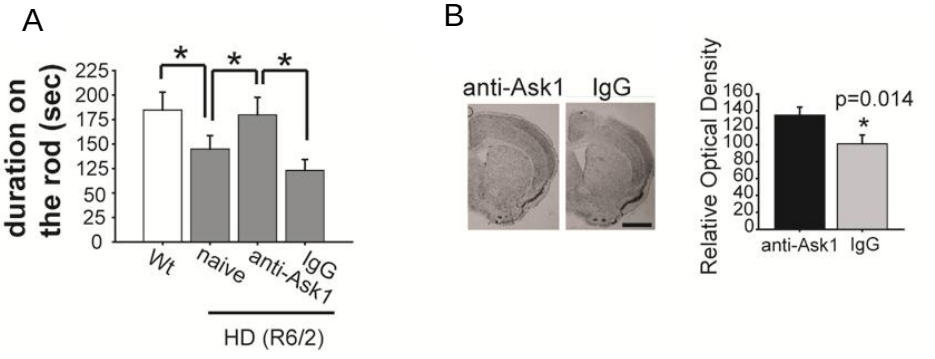

Figure 6. The effect of inhibition of Ask1 on expression of motor dysfunction. (A) Motor function was evaluated as the amount of time spent on the rotarod. HD mice were not able to remain on the rod for long periods of time, but Ask1-inhibited HD mice remained on the rotarod longer than vehicle-treated mice. There was no significant difference in motor performance between naive HD mice and vehicle-treated HD mice. cor, cortex; str, striatum; *p < 0.01. **(B)** Inhibition of Ask1 prevents striatal atrophy. Representative photographs of brain sections from Ask1 antibody-treated or IgG/preimmune antibody-treated HD mice ; Sizes of the striatal area and ventricle in Ask1 antibody-treated HD mice (anti-Ask1) and IgG/preimmune antibody-treated HD mice (IgG). Scale bar = 500 μm; *p = 0.014.

IV. DISCUSSION

In this study, we presented two novel findings suggesting that increased Ask1 may play a critical role in HD progression in mice. First, we showed for the first time *in vivo* that the level of Ask1 protein is increased in HD (R6/2) mice, as is ER stress. Second, we demonstrated that inhibition of Ask1 prevents the translocation of htt fragments and improves motor dysfunction in mice, suggesting that Ask1 may be closely correlated with disease development in HD mice.

Our findings indicate that Ask1 is an element in ER stress-triggered neuronal cell death in a HD animal model (Figure 1). This finding is consistent with a study performed in a cell culture system that showed that Ask1 mediates proteasome dysfunction and ER stress-induced neuronal cell death by neuropathological alterations in polyQ disease [3]. Moreover, the levels of Ask1 protein and CHOP transcripts were greater in the cortex than the striatum of HD mice (Figure 1). Our study showed that the level of Ask1 protein was increased in the cortex and striatum of HD mice (Figure 1). Based on our previous study of Ask1 [14], phosphorylation of Ask1 is required for its activation, but if insufficient Ask1 protein is present, cell death may not be initiated. Normal htt is balanced with the pro-apoptotic role of the N-terminal mutant htt fragments [20]. However, expansion of the htt fragments could disrupt this balance because of the sustained presence of htt fragments. In HD, loss of intact htt along with accumulation of htt fragments may move the cell towards a toxic state [21], which is known to damage corticostriatal projection neurons thereby reducing growth factors such as BDNF in the cortex. Finally, reduced BDNF transport from the cortex to the striatum may result in the death of striatal cells and behavioral abnormalities [5]. In the present work, we demonstrated that intact htt was reduced to a greater extent in HD than in wt mice, and that levels of htt are

lower in the striatum than in the cortex of HD mice (Figure 2), suggesting that htt fragmentation may occur to a greater extent in the striatum of HD mice. Furthermore, the vast majority of htt fragments was detected in the cytoplasm (Figure 2), consistent with previous reports that cytoplasmic htt cleavage precedes nuclear uptake [20,21].

Ask1 activity, as assessed by the amount of pAsk1 (Thr845) present, was effectively inhibited in both the cortex and striatum of the Ask-1 antibody-treated group compared to the control group (Figure 3). Because Ask1 antibody was infused in the striatum, Ask1 activity was scarcely detected in the striatal fraction in contrast to the cortical fraction. When Ask1 activity was inhibited (Figure 3), CHOP induction decreased significantly. Inactivated Ask1 binding to htt fragments was mainly detected in the cytosolic fraction of cortical cells, as shown by the immunoprecipitation and double-immunohistochemistry experiments (Figure 4). Larger htt fragment do not readily enter the nucleus [22], and the translocation of htt fragments to the nucleus is associated with increased htt toxicity *in vitro* and neuropathology *in vivo* [20]. Because caspases interact with htt and produce cytotoxic htt fragments, the interaction of caspases and htt amplifies caspase activation and initiates the caspase cascade in the brains of patients with HD [20,22]. We speculate that Ask1 may recruit caspases thereby facilitating htt fragmentation. In future studies, we plan to investigate this hypothesis. Alternatively, Ask1 in the normal state may act as a type of chaperone and help the smaller htt fragments enter the nucleus, but when inhibited, might bind to htt fragments in the cytosol and hinder the translocation of htt fragments into the nucleus. Based on our results, we suggest that Ask1 is a key modulator of cellular signal transduction in R6/2 HD mice. Ask1 has a dual role: it is activated by various harmful stimuli and simultaneously activates or binds to other cellular molecules. We suggest that Ask1 is activated by ER stress

and that active Ask1 interacts with htt fragments, allowing them to translocate into the nucleus more efficiently. This interaction may amplify ER stress and may contribute to an htt toxicity feedback loop. This interaction may be one of the explanations why ER stress was reduced in Ask1 antibody-treated HD mice. We speculate that Ask1 positively regulates ER stress rather than simply respond to the ER stress signal. Under the condition of continuous ER stress, ER stress-induced neuronal cell death could be suppressed by BDNF-mediated neuroprotection [23,24]. Prevention of BDNF protein reduction by inhibition of Ask1 could be inferred to suppress CHOP expression, which may supply another explanation for positive regulating role of Ask1 in CHOP.

In HD pathogenesis, the hypothesis that dysfunction of the corticostriatal pathway may contribute to the onset of HD has been supported by the observation that BDNF is expressed in cortical neurons and delivered to striatal neurons [25]. BDNF co-localizes with htt in cortical neurons that project to the striatum [5]. In this study, when Ask1 was inactivated in the striatum, the levels of BDNF protein in the cortex increased compared to preimmune antibody-treated HD mice, although there was no difference in the expression level of BDNF transcripts. These findings imply that inactivated Ask1 modifies the levels of BDNF protein at the post-translational level. Because cortex-specific deletion of BDNF is known to elicit progressive striatal degeneration in mice [25], BDNF reduction is expected to contribute to striatal pathogenesis in HD. Although striatal toxicity caused by htt fragments alone can not explain progressive locomotor deficits [26], our rotarod test results demonstrate that inhibition of Ask1 activity in the striatum can alleviate motor dysfunction symptoms in HD mice (Figure 6). Along with the improvement in motor dysfunction, striatal atrophy was decreased in Ask1 antibody-treated HD mice compared to that in naïve HD and IgG/preimmune antibody-treated HD mice (Figure 6).

V. CONCLUSION

In this study, we demonstrated that ASK1 was involved in the translocation of small htt fragments into the nucleus rather than htt cleavage. Increased levels of Ask1 may interact with htt fragments and subsequently induce ER stress. ER stress can be diminished by inhibiting Ask1, resulting in prevention of BDNF depletion in the striatum and an improvement in behavioral and anatomical abnormalities. Therefore, regulating the amount and activity of Ask1 protein are promising novel treatment strategies for HD.

PART II

Apoptosis signal-regulating kinase-1 aggravates ROS-mediated striatal degeneration in 3-nitropropionic acid-infused mice

I. INTRODUCTION

The compound3-nitropropionic acid (3-NP) produces selective striatal lesions in animal models [27]. Although not entirely elucidated, the mechanisms of neurotoxicity induced by 3-NP have been shown to include the exhaustion of adenosine triphosphate, mitochondrial membrane depolarization, dysregulation of intracellular calcium homeostasis, calpain activation, and the release of pro-apoptotic proteins from mitochondria [28-30]. The neurotoxic mechanism and the reason for the selective vulnerability of the striatum are not yet well understood.

Superoxide dismutase (SOD) functions to protect cells from the effects of superoxide radicals by eliminating reactive oxygen species (ROS). Several reports have shown that SOD overexpression reduced the size of striatal lesions after 3-NP injection [31]. Increased cytosolic Cu/ZnSOD is a compensatory response to the generation of ROS to reduce the toxic effects of the superoxide anion. In addition, the cumulative effects of ROS exposure cause the activation of various harmful cellular pathways [32-34].

Apoptosis signal-regulating kinase-1 (ASK1), an early signaling element in the cell death pathway [35], is activated by ROS [36] and is required for ROS-induced apoptosis [37]. Previous studies have indicated that increased activated ASK1impacts the presentation of neurodegenerative diseases [10,12].The rationale for targeting ASK1 was based on findings that oxidative stress is causally related to apoptotic neuronal cell death in neurodegenerative lesions commonly associated with abnormal protein fragments and aggregates [34,38]. Although many investigations have shown that ASK1 is essentially involved in neuronal cell death triggered by various external injuries and expanded polyglutamine, the relationship of ASK1 and ROS in the selective striatal cell

death by 3-NP chronic and systemic infusion in mice remains is to be elucidated. In addition, ASK1 was suggested to play a role in mediating the cell death signal in striatal cells of aged mice that received 3-NP injections directly into the striatum.

Here, we examined whether increased levels of ASK1 are reciprocal to the amount of ROS and also investigated the relationship between ASK1 expression and striatal degeneration in 3-NP systemic infusion mice. We suggest that overexpressed ASK1 amplifies ROS damage, which can lead to cell death, and is a deleterious primary responder to oxidative stress in the striatum of 3-NP systemically infused mice.

II. MATERIALS AND METHODS

1. Animal model

Male SOD1-tg mice (C57BL/6-TgN; Jackson Laboratory, USA) and wild type (wt) male littermates were used in this study. All procedures were performed in accordance with the guidelines for the care and use of laboratory animals (Yonsei University), which have been approved by the Association for Assessment and Accreditation of Laboratory Animal Care (AAALAC). The animals were anesthetized with 2.0% isoflurane under 30% oxygen and 70% nitrous oxide using a vaporizer (VMC Anesthesia Machine, MDS Matrix, USA). The rectal temperatures were maintained at 37 ± 0.5℃. For the sustained chronic administration of 3-NP infusion, 3-NP (Sigma, USA) was dissolved in saline at a concentration of 0.5 mg per μl (pH 7.4). The prepared 3-NP solution or vehicle control was delivered by sustained infusion (180~220 mg/Kg/day) using osmotic mini-pump at an infusion rate of 0.5 μl/h for 7 days (Alzet, USA).

2. ASK1gene silencing with siRNA and Administration of ASK1-peptide

The ASK1 gene was silenced using siRNA against ASK1 (sense, GCUCGUAAUUUAUACACUGtt; antisense, CAGUGUAUAAAUUACGAGCtt; concentration 5 μM; Ambion, Austin, TX, USA). After confirmation of efficiency *in vitro*, the transfecting reagent SiPORT*Neo*FX (Ambion, USA) and ASK1-siRNA or nonfunctional mutantRNA (control siRNA; 5'-AAG AGA AAA AGC GAA GAG CCA-3'; Ambion) were combined, mixed gently, and allowed to form siRNA liposomes for an additional 10 min at room temperature. An alzet micro-osmotic pump (Durect, USA) containing 100 μl of the transfection reagent or ASK1-siRNA

was then placed subcutaneously on the backs of the animals, and a brain infusion cannula connected to the pump was positioned in the striatum (A, 0.7 mm; L, 1.2 mm, and D, 3.3 mm) for 7 days during 3-NP infusion. The mice were sacrificed 7 days after surgery, and the brains were processed for experiments.

To restore ASK1, we synthesized an ASK1 peptide containing active sites (Thr845) from amino acids 836 to 875. The ASK1 protein was transported with the dried BioPORTER Quiktease (Sigma Aldrich) reagent to the striatum of SOD tg mice concomitant with 3-NP infusion for 7 days by a micro-osmotic pump containing 100 μl of ASK1 protein (0.1 mg/ml in saline). As a control, control-peptides were infused in the 3-NP-infused SOD-tg mouse striatum. To confirm the delivery, western blot analysis was performed with antibodies recognizing the Thr845 region.

3. Immunohistochemistry

To determine thepatterns of DARPP32 (Epitomics, USA) and ASK1 (SantaCruz Biotechnology, Cell signaling) expression, we performed immunofluorescent staining. After sacrificing the animals, brains were removed, fixed, and cut into 20μm thickness coronal sections on a cryostat. The fixed sect ions were incubated with a blocking solution, as described previously [39], a nd incubated with the appropriate primary antibodies. After washing, the sections were incubated with fluorescein isothiocyanate (FITC)-conjugated secondary antibodies (Jackson ImmunoResearch, USA). For counter-staining, the sections were incubated with propidium iodide (PI, Sigma). After washing, stained tissue samples were mounted using Vectashield mounting medium (Vector Lab, USA) and coverslipped. The sectionswere then observed under a LSM510 confocal laser scanning microscope (Carl Zeiss, USA).

4. Western blot analysis

The protein expression levels were analyzed by western blotting. Tissues were lysed in lysis buffer (20 mM Hepes–KOH, pH 7.5, 250 mM sucrose, 10 mM KCl, 1.5 mM $MgCl_2$, 1 mM EDTA, 1 mM EGTA, 0.5mM PMSF, 0.1mMsodium vanadate, 0.1mM proteinase inhibitor cocktail), the samples were homogenized with a Teflon homogenizer (Wheaton, USA), and then centrifuged at 8,000 *g* for 20 min. The lysates were loaded onto SDS-polyacrylamide gels and after migration, the proteins were electro-transferred onto a polyvinylidenedifluoride membrane (PVDF) (Millipore, USA), which was then blocked in 5% skim milk and incubated with one of the following primary antibodies: Cu/ZnSOD, MnSOD, ASK1, pASK1. After washing, the blots were incubated with horseradish peroxidase-conjugated secondary antibodies (Roche Diagnostics), and the bands were visualized with an enhanced chemiluminescence reagent (Amersham Biosciences).

5. Apoptotic cell-death assay

Apoptosis-related DNA fragmentation assays were quantified using a commercial enzyme immunoassay kit (Chemicon) and cytoplasmic histone-associated DNA fragment kit (Roche Diagnostics). According to the manufacturers' protocols, cytosolic samples were used in each assay. In addition, we performed a TUNEL assay to detect cell death following the manufacturer's protocol (Roche Diagnostics)**.** Tissue were prepared as described above, and immune-fluorescent labeling was performed as previously described [40,41]. The sections were incubated with 50 l of the TUNEL reaction mixture, and the sections were counterstained with Hoechst (Molecular Probe, USA), mounted, and observed under a confocal laser scanning microscope (Carl Zeiss). The number of TUNEL-positive cells was counted in the striatum in three sections

from each mouse at different levels.

6. ROS detection by staining

ROS were investigated in the brains of 3-NP-infused mice using green-fluorescence (CM-H_2DCFDA) *in situ* detection (Molecular Probes). Each mouse was placed in a stereotaxic frame (Stoelting) under general anesthesia, the CM-H_2DCFDA (2 ul, 50ug/50ul dimethylsulfoxide) was infused for 10min into the striatum with a Hamilton syringe. The animals were sacrificed and trans-cardially perfused with heparin and formaldehyde 1h after infusion of CM-H_2DCFDA. After preparing a frozen block of brain tissue, ROS was detected to appear as green dots by CM-H_2DCFDA when examined under confocal laser scanning microscope (Carl Zeiss).The nucleus was stained with PI (Sigma).

7. ROS detection by flow cytometry analysis

CMXRosamine (MitoTracker-Red™) and CMH_2-DCFDA (Molecular Probe) were obtained from Molecular Probes, dissolved in DMSO, and stored at 20℃ in the dark. Both MitoTracker (50 μM) and CM-H_2DCFDA (50 μM) were administered into the cortex and striatum at the position described above 30 min before sacrifice. As a control, DMSO was injected in the same locations at the same time before sacrifice in some mice. Following this procedure, the mouse brain was removed, dissected out striatum, and minced finely with a scalpel. Minced striatum tissue was placed in separate tubes containing 2 ml digestion solution, and cells were dissociated with Accumax (Millipore) for 1 h at 37℃ with agitation in the dark. The cell suspension was filtered through a 100-μm mesh (BD Biosciences) and diluted with PBS after fixing the single cells with 3.7% formaldehyde in the dark, the fluorescence of the bound dyes within each

cell was analyzed using a FACSCalibur (BD Biosciences; over 100,000 total events; 5,000 events / gate), and the data were analyzed using Cell Quest software (version 3.3; BD Biosciences). Negative controls were prepared by reacting the tissues with PBS, FITC-conjugated IgG, or PE-conjugated IgG (BD Biosciences).

8. Detection of DNA oxidation in mouse striatum

We evaluated DNA oxidation usinga monoclonal antibody against 8-OHdG according to a previous report [32]. The brain tissue was fixed, and treated with DNase-free RNase (Roche) at 37℃ for 1 h. Next, the sections were denatured in 4N HCl and neutralized with 50 mM Tris-base. After washing, the samples were incubated with an anti-mouse 8-OHdG antibody and also incubated with secondary antibody (MOM kit, Vector Laboratory, USA). The slides were mounted with Vectashield and coverslipped.

9. Rotarod test

The motor function of the animals was assessed with a rotarod apparatus (UgoBasile, USA), where the time that the animals were able to remain on the rod was measured at an accelerating speed from 4 to 40 rpm. Each mouse was pre-trained before implanting the osmotic pump filled with 3-NP or saline. After 30min rest period, and mice were then placed back on the rotarod for five trials of a maximum of 5 min at an accelerating speed.

10. Statistical analysis

Data are expressed as the mean ± SD. The statistical comparisons among multiple groups were performed using analysis of variance followed by Fisher's *post hoc*protected least-significant difference test, and comparisons between

two groups were performed using the unpaired *t* test (StatView, version 5.01; SAS Institute Inc., Cary, NC, USA).

III. RESULTS

1. Systemic infusion of 3-NP led to the formation of selective striatal lesions in wt, but SOD-tg mice

Mice infused with 3-NP were examined for symptoms, and the degenerated brain region was validated with cresyl violet staining. Primarily, we confirmed an obvious decrease in body weight by 7 days after systemic3-NP reservoir implantation. The mouse body weight reduced an average of 70% of the initial body weight. Seven days after 3-NP administration, most mice presented with severe motor dysfunction in addition to weight loss. Histological evaluation of the 3-NP-infused mice at day 7 demonstrated striatal abnormalities and cell loss (Figure 1A).

DARPP32 (dopamine- and cyclic adenosine monophosphate-regulated phosphoprotein), an established of striatal neuron marker, showed weak immunoreactivity in 3-NP-infused wt mice; however, the immunoreactivity in SOD- tg mice was significantly more dense (Figure 1B). The induction of DNA damage in striatal neurons was evaluated by terminal TUNEL staining (Figure 2). The average number of TUNEL-positive nuclei was determined using multiple images in the four different mice of each group. Figure 2 reveals a statistically significant increase in TUNEL-positive nuclei in the 3-NP-infused wt mice, which was scarcely demonstrated by the DARPP32-positive cells.

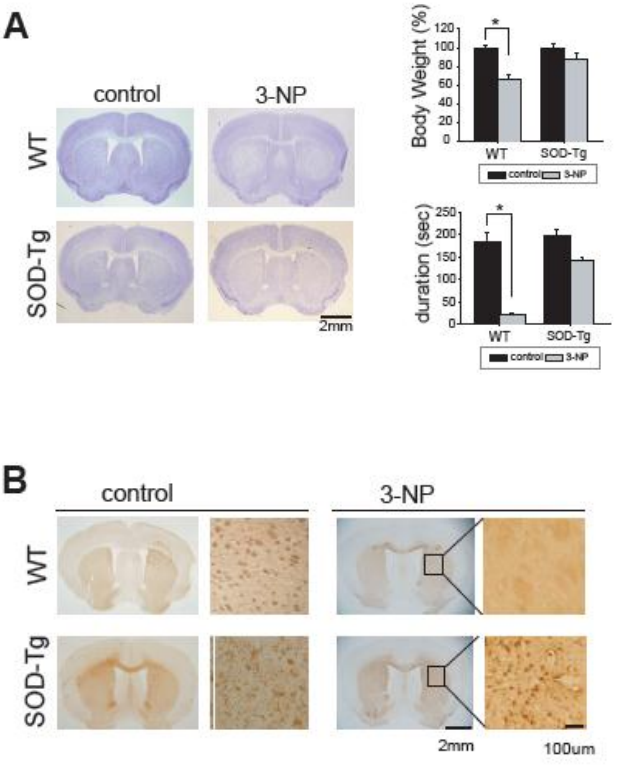

Figure 1. Pathological examination in the striatum after systemic infusion of 3-NP. (A) Histological analysis was performed by cresyl violet staining (left). Body weight which measured on day 7 after infusion of 3-NP is expressed as a percentage of the weight before 3-NP infusion (right upper). Motor function is shown the duration sustained on the rotarod (right lower). **(B)** DARPP32-postive cells shown by immunohistochemistry was sparsely detected in the wt mice, while positive cells were more plentiful in the SOD-tg.

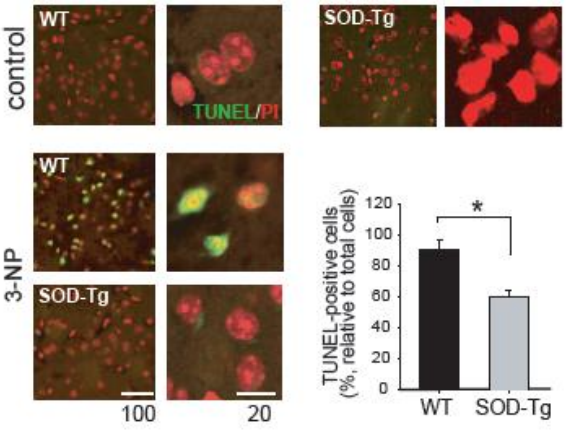

Figure 2. Apoptotic cell death in wt and SOD-tg mice. TUNEL-positive cells were more densely detected in the 3-NP-infused wt mice compared to the SOD-tg mice (left). A quantification graph is presented showing relative values of positive cells to counterstained cells in the unit area (right). *p<0.05.

2. Greater ROS production, oxidative damage and ASK1 levels and activity were detected in striatal lesions

Using FACS analysis to quantify ROS, the total amount of ROS in the striatum significantly decreased from 9.57% in wt to 28.75% of SOD-tg mice (Figure 3). In contrast, there was a slight difference in the ROS quantity in mitochondria that were directly injured after 3-NP infusion between wt and SOD-tg mice (Figure 3), as revealed by FACS (wt, 99.99%; SOD-tg, 81.37%).

As an alternative way to compare the changes in the amount of ROS, levels of MnSOD, and Cu/ZnSOD proteins, were determined by western blot analysis in the lesioned striatum from each brain. MnSOD protein amounts were not different in the damaged striatum between wt and SOD-tg, whereas relatively higher levels of Cu/ZnSOD were detected in SOD-tg than wt (Figure 4). Unaltered pattern of MnSOD likely dues the direct attack of the mitochondrial dysfunction reagent, 3-NP. Cytosolic SOD levels, however, were greater in the SOD-tg than in the wt mice because of the restoring effect of SOD overexpression in the SOD tg mice.

Representing DNA oxidation, 8-OHdG-positive cells were scarcely detected in the 3-NP-infused SOD-tg striatum; however, the immune-reactivity was strong in striatum of wt mice (Figure 5), suggesting that the ROS was produced following mitochondrial dysfunction and subsequent DNA damage (Figure 6). Under oxidative conditions, increased ASK1 protein levels, one of the first ROS-responsive molecules, were measured, and also measured increased pASK1 activated by phosphorylation at Thr845. The 3-NP infusion elevated total ASK1 protein amounts the SOD-tg and wt mice however, this increase was meager in the SOD-tg group. Corresponding to total ASK1 amounts, the levels of pASK1 were also significantly lower in SOD-tg mice (Figure 2D).

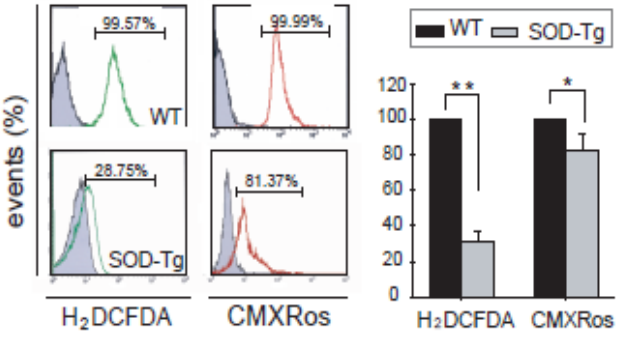

Figure 3. Environmental changes and ROS level changes in the striatum after 3-NP infusion. After 3-NP infusion, CM-H_2DCFDA-for evaluating total ROS levels, and MitoTracker-Red for mitochondrial ROS levels were assayed by flow cytometry (left), and the events are presented in a quantified graph (right).

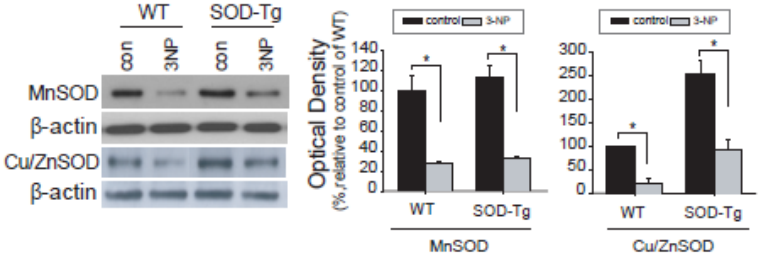

Figure 4. The alteration of ROS scavenging enzyme protein level in the striatum of wt and SOD tg mice after 3-NP infusion. The MnSOD and Cu/ZnSOD protein levels in the striatum are shown in western blot analysis (left) and the quantitative values are presented in the graphs (right).

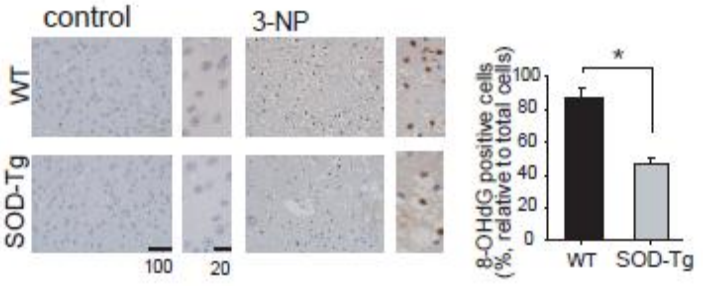

Figure 5. Oxidative DNA damage in the striatum of wt and SOD tg mice after 3-NP infusion. The 8-OHdG illustrates that the 8-OHdG-positive cells were more densely detected in the wt mice compared to the SOD-tg mice. A quantified graph is presented showing relative values of positive cells to counterstained cells in the unit area.

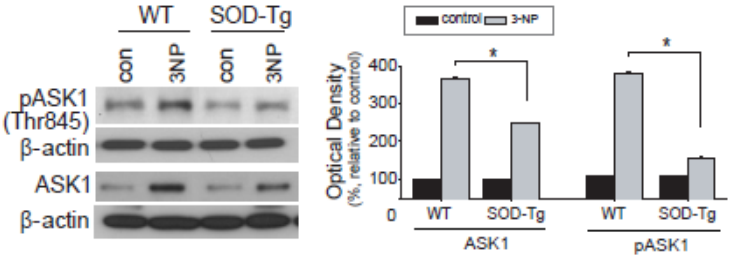

Figure 6. The changes of ASK1 protein and activity. The changes of ASK1 and pASK1expression levels were assayed by western blot (left) and presented the quantified graph (right). *p<0.05.

3. ASK1 amounts mediated the striatal cell death without change of ROS level

ASK1 gene silencing by siRNA sufficiently regulated ASK1 protein down (Figure 7). However, ASK1 silencing did not alter the amounts of ROS by 3-NP infusion. Indeed, ROS levels were similar or abundant both in the si-ASK1-treated and the si-control-treated wt mice. ROS detected with CM-H_2DCFDA were scant in 3-NP-infused SOD-tg mice, while the CM-H_2DCFDA in normal and ASK1-silenced 3NP infusion mice abundantly stained the striatal region with a punctuate shape (Figure 7). The results showed that the down-regulation of ASK1 did not affect ROS generation. Although the down-regulation of ASK1 did not affect ROS scavenging, it was sufficient to reduce cell death and improve the motor function (Figure 9). On the other hand, ASK1-peptide administration triggered cell death without increasing ROS levels.

To confirm whether overexpression of ASK1 plays a role in mediating cell death, synthesized ASK-peptide was infused for 7 days in the SOD-tg mice striatum starting with 3-NP systemic infusion (Figure 8). In 3-NP-infused SOD-tg mice, the ROS levels were assessed in the control-peptide and ASK1-peptide treated groups by FACS (Figure 8). ASK1-peptide did not alter the amount of ROS generated. A DNA fragmentation assay showed that striatal apoptotic cell death occurred in the 3-NP-infused wt mice and decreased significantly in both SOD-tg mice and siASK1-treated wt mice with 3-NP infusion. In contrast, the DNA fragmentation recurred in the ASK1-peptide-treated SOD tg mice and also aggravate movement ability (Figure 9).

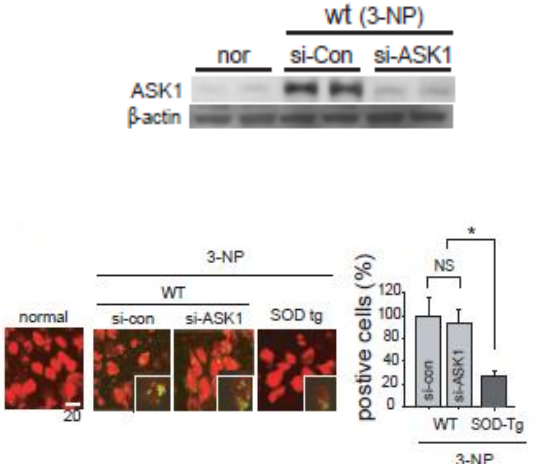

Figure 7. Down regulation and induction of ASK1. In the striatum, ASK1 proteins were declined by siRNA-ASK1 (left), and quantified graph (right). CM-H_2DCFDA in the striatum was detected in abundance in the si-control- or si-ASK1-treated wt mice, but was decreased in the 3-NP-infused SOD-tg mice. H_2DCFDA**,** green; PI, red.

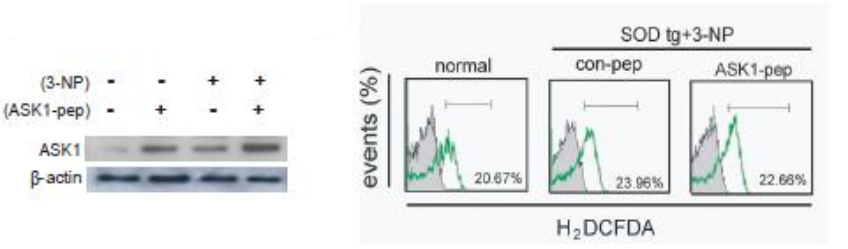

Figure 8. The effect of ASK1-peptide on ROS production level. Western blot analysis shows the expression levels of ASK1 in the striatum of wt or ASK1-peptide-added SOD-tg mice with 3-NP infusion. After 3-NP infusion, total ROS levels was evaluated with CM-H_2DCFDA in each group (con-pep vs ASK1-pep) by flow cytometry.

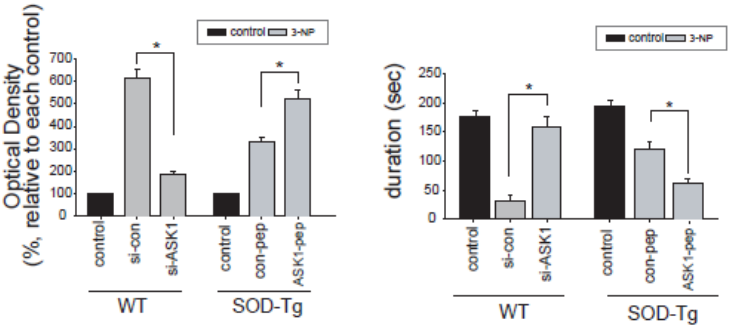

Figure 9. The role of ASK1 in cell death and behavioral impairment. Apoptotic cell death using DNA fragmentation assay was found in each treated mouse striatum. Motor function is shown as the duration sustained on the rotarod in each treated group. *p<0.05.

IV. DISCUSSION

The results of the present work show an improvement in behavioral impairment by ASK1 down-regulation, despite 3-NP infusion. We propose the hypothesis that ASK1 overexpression by systemic infusion of 3-NP promotes the formation of selective striatal lesions, and this occurs apart from ROS generation. The results of our study showed that increased ASK1andpASK1expression by harmful ROS signals augmented neuronal cell death in the striatum.

Mitochondria are key players in the production of ROS and have been reported to have an important role in 3-NP injury-induced pathology [42]. We evaluated amounts of total ROS produced in mitochondria and cytosol MitoTracker-Red CMH_2XRos (MT Red CM-H_2XRos) is a molecule that has been used to measure mitochondrial free radicals (MFRs) in various cell cultures. Because this dye has been reported to be sequestered into the nucleus and vesicles [43,44], we administered it to detect the generation of MFRs in 3-NP-infused mice and to measure MFR generation *in situ.* Besides of mitochondrial dysfunction, 3-NP also raises cellular oxidative stress. The alteration of Cu/Zn-SOD is a compensatory mechanism that protects cells from free radical-induced damage, and systemic infusion of 3-NP altered Cu/Zn-SOD enzyme levels in this study. It has been previously reported that 3-NP induced major changes in SOD activity in the striatum of 3-NP-injected rats [45]. Our study displayed that 3-NP caused a reduction in Cu/Zn-SOD, but had no effect on MnSOD protein levels. It can be inferred that the overexpression of Cu/ZnSOD is primarily responsible for cellular anti-oxidant protection in 3-NP-infused SOD-tg mice, possibly by compensating for the overexpression of ROS. In wt mice, however, the endogenous antioxidant system could not enough to eliminate the increased ROS, as Cu/ZnSOD amounts were

diminished. The lesions of 3-NP indicate that striatal oxidative damage has occurred, and that this damage is associated with changes in the cellular antioxidant system [46]. The Cu/ZnSOD levels were much greater in the SOD-tg mice compared to the wt mice, likely to overcome the oxidative damage. However, the changes in SOD protein levels during oxidative stress do not determine whether protect or not, although it is certain that overexpressed SOD amounts protect against harmful oxidative environments [33].

Oxidative DNA damage results from direct ROS attacks. There are some types of oxidative DNA damage detective method. Among them, 8-OHdG results in oxidative DNA damage. The results presented here show that the oxidative DNA lesions are markedly augmented in the 3-NP-infused wt mouse brain.

Once ROS are generated, they can damage mitochondria causing additional free-radical generation and loss of antioxidant capacity, leading to a deleterious cycle [4]. Therapeutic prevention of oxidative stress has been proposed to "break the cycle" of cell death [4], and studies have been carried out in the neurodegenerative field attempting to modulate key enzymatic components that regulate oxidative stress [33]. Our study was performed on the assumption that mitochondrial complex II inhibitors generate ROS, and contribute to cell death. Furthermore, because ASK1is known to be involved in ROS-induced cell death, we propose that ASK1plays an instrumental role and even amplifies this process. The ASK1 signaling-mediated cell fate decision appears to depend in part on the extent and duration of ASK1 amounts and its activation. A previous report found that a mutated SOD induced ER stress and activated the ASK1-mediated cell death pathway [13]. Also, the deletion of ASK1 mitigated neuronal loss and extended the life span of SOD1-mutated mice [13].

Recent studies with animal models have revealed that oxidative stress is a

causative factor in the initiation and progression of Alzheimer's disease (AD) and Parkinson's disease, where antioxidants have the capacity to attenuate the phenotypes associated with these neurodegenerative disorders. Although antioxidants can prevent the oxidative stress-mediated progression of neurodegenerative diseases [47], antioxidant treatment is not sufficient to halt disease progression. We implied that inhibition of ASK1, the major downstream activator, may disrupt the positive feedback Therefore we propose that mitochondrial dysfunction by 3-NP induces an increase in ROS level; ROS-activated ASK1 mediates harmful oxidative signals; and cells eventually undergo apoptosis. The precise mechanisms have not yet been elucidated and have to be investigated.

V. CONCLUSION

This study is summarized as followings: (1) systemic infusion of 3-NP increased ROS and led striatal cell loss; (2) ASK1 down-regulation decreased striatal cell death without scavenging ROS; (3) adding ASK1protein to SOD tg aggravated striatal degeneration; and (4) ASK1 activation induced by ROS is an important step of the 3-NP pathophysiology. Conclusively, this study indicates that ROS-induced ASK1 is an important step in the pathogenesis of 3-NP-mediated striatal lesion, and suggests that ASK1 acts as an amplifier of the ROS signal cascade. Taken together, we suggest a combination of ASK1 inhibition and ROS elimination for more effective therapy.

PART III

Apoptosis signal-regulating kinase 1 mediates 3-nitropropionic acid toxicity and regulates C1q level via astrocyte TGF-beta

I. INTRODUCTION

The systemic administration of 3-nitropropionic acid (3-NP) facilitates the development of selected striatal lesions and it remains unclear whether specific neurons are selectively targeted in 3-NP infused striatal degeneration. It is well known that 3-NP inhibits succinate dehydrogenase (SDH), mitochondrial complex II, to the same extent in both the cerebrum and the striatum [4,25], suggesting that 3-NP neurotoxicity occurs to the same extent in the cerebrum and the striatum. Although not entirely elucidated, the mechanisms of neurotoxicity induced by 3-NP have been shown to include the exhaustion of adenosine triphosphate, mitochondrial membrane depolarization, dysregulation of intracellular calcium homeostasis, calpain activation, and the release of pro-apoptotic proteins from mitochondria [28,30,48]. The neurotoxic mechanism and the reason for the selective vulnerability of the striatum are not yet well understood. 3-NP has been used a pharmacologic model to study mitochondrial dysfunction in relation to Huntington's disease (HD). However, speculation of selective regional neurotoxicity induced by 3-NP in different areas may not be accurate, and the molecular mechanisms underlining 3-NP-induced striatal lesion remain to be fully defined [49].

Mitochondrial dysfunction can bring energy metabolism defects, oxidative stress, and defects in mitochondrial calcium usage. A number of studies have examined whether alterations in mitochondrial respiration contribute to the observed bioenergetic defects. Biochemical studies of brain and peripheral tissues from HD patients, as well as studies on HD cells and animal models, revealed decreased activity of several enzymes involved in oxidative phosphorylation such as complex I, II, III, and IV [23,27,50-52]. Mitochondria are both a target and an important source of reactive oxygen

species (ROS). Although data on post mortem tissues show contrasting results on the presence of oxidative stress products [53], further analyses in animal models of HD, and systemic injection of 3-NP suggest that oxidative stress may play an important role in the pathogenesis of HD [54]. It was found that pathways by which cellular energy is lost are clearly different in 3-NP-treated neural cells versus the same cells bearing the expanded polyglutamine tract of the HD protein, suggesting that mitochondrial defects may be a consequence of neurodegeneration [55]. To relate with mitochondrial morphology, 3-NP did not induce translocation of the dynamin-related protein 1 (Drp1) to the mitochondria, and the Drp1 inhibitor Mdivi-1 did not affect the observed changes in mitochondrial morphology [56]. Also, scavengers of ROS failed to prevent mitochondrial alterations. It shows a direct correlation that formation of mitochondrial permeability transition pores and autophagy induced by 3-NP treatment. Activation of autophagy preceded the apoptotic process and was mediated, at least partly, by formation of ROS and mitochondrial permeability transition pores. Superoxide dismutase (SOD) has function to protect cells from the effects of superoxide radicals by eliminating ROS. Several reports have shown that SOD overexpression reduced the size of striatal lesions after 3-NP injection [31].

Apoptosis signal-regulating kinase-1 (ASK1), an early signaling element in the cell death pathway [35], is activated by ROS [36] and is required for ROS-induced apoptosis [37]. Previous studies have indicated that increased activated ASK1impacts the presentation of neurodegenerative diseases [12]. The rationale for targeting ASK1 was based on findings that oxidative stress is causally related to apoptotic neuronal cell death in neurodegenerative lesions commonly associated with abnormal protein fragments and aggregates [34,38]. Although many investigations have shown that ASK1 is essentially involved in

neuronal cell death triggered by various external injuries and expanded polyglutamine, the relationship of ASK1 and ROS in the selectively striatal cell death by 3-NP chronic and systemic infusion in mice remains is to be elucidated. In addition of cell death initiation resulted from increased ASK1, depletion of neurotropic factor BDNF is major cause of striatal degeneration. Mitochondrial dysfunction alone is insufficient to elicit the striatal gene expression phenotype of HD, which the current report suggests the putative pathway generate striatal degeneration. Many experimental results derived from both clinical as well as basic research suggest a close correlation between BDNF deficiency and HD pathogenesis [49]. In metabolic compromise, neurodegeneration caused by 3-NP involves three interacting processes. The main causes are energy impairment, excitotoxicity, and oxidative stress, which are related to HD pathogenesis [49]. As report that examined the striatal gene expression in the both heterogygous and homozygous BDNF knock-out models is more like human HD than the other HD models, the results implicates that reduced trophic support as a major pathway contributing to striatal degeneration in HD [57].

C1q is a component of the complement initiator C1 complex. During development, C1q is expressed in synaptic regions of developing postnatal CNS [58]. Depending on the timing and local environment, the complement cascade can facilitate proper neuronal development or accelerate chronic inflammatory response contributing to neurodegeneration. Induced synthesis of C1q in the CNS has been seen in several injury models, such as viral infection [59], kainic acid treatment [60], stroke [61], and in hippocampal organotypic slice cultures stimulated with β-amyloid (Aβ) [62]. In blood, C1q is normally present in complex with proenzymes C1r and C1s as the C1 macromolecular initiator of the classical complement pathway [63]. The C1q response is biphasic. In stroke model, it was reported that increased C1q drove two independent

pathophysiological mechanisms involved in the processes of lesion formation and BBB disruption. (1) Excess C1q may lead to increased functional active C1, and resulted in increased activation of the classical pathway. (2) C1q is known to trigger a number of receptor-mediated cellular effects, even in the absence of downstream complement activation, and any of these might contribute to tissue injury [64]. C1q plays a role as a pattern recognition receptor [65] that mediates the clearance of cells undergoing cell death by apoptosis [66], and can enhance the uptake of apoptotic cells [67]. Exogenous plasma C1q, therefore, may play a role in the initiation of cell activation in microglial cells in the course of CNS diseases with blood-brain barrier impairment and may contribute in an autocrine or paracrine way to maintain and balance microglial activation in the diseased CNS tissue [68]. Neuronal C1q expression is downregulated in the CNS in adulthood. Knock-out mice lacking C1q are characterized by large, sustained defects in CNS synapse elimination. Stevens et al proposed that complement-mediated synapse elimination may be aberrantly reactivated in neurodegenerative disease [69].

Our previous results showing that striatal excitotoxic lesions differentially regulated molecules in each brain region suggest that changes in the levels of ASK1 including BDNF, could underlie the differential vulnerability of striatal neurons observed in 3-NP infusion or HD mice. The main goal of the present study is to characterize the regulation of BDNF in each subregion, cortex and striatum. The current study investigates that mild and chronic exposure of mitochondrial toxin can modulate the C1q level both in cortex and striatum via regulation of TGF-beta from astrocyte. Consequently we investigate how the BDNF is dominantly depleted in striatum, and finally whether striatal lesion is established in relating to ASK1 pathway.

II. MATERIALS AND METHODS

1. Primary neuronal cell culture

Primary cortical or striatal neurons were cultured with mouse pups and culture procedures are based on the widely used, non-feeder layer–based (without astroglial feeder cell layer). Embryonic day 14 pups were removed from the pregnant mother mouse. Cortex was dissected in Hank's buffered salt solution (CMF-HBSS) and tissues were digested with 2.5% trypsin for 12 min in a 37℃ water bath. The supernatant was removed, rinsed with three successive washes of HBSS and resuspended in neurobasal media (NB, Life Technologies) contained 0.2 mM GlutaMAX (Life Technologies) and 2.0% B-27 Supplement (Invitrogen). Cells were subsequently plated on 12 mm glass coverslips (Bellco) in 24 multi-well plates, pre-coated with 1 mg/mL poly-L-lysine (Sigma) at a density of $5x10^4$ cells per mL. Neurons were subsequently incubated at 37℃ with 5% CO_2 and remained in culture for 15 days *in vitro* (*DIV*) to allow for the development and maturation of dendritic spines. Every 3–4 days, the neurons were fed by replacing one half of the fresh NB media.

2. Animal model and lesion analysis

In this study, male C57BL/6J mice were used and male SOD1-tg mice (C57BL/6-TgN; Jackson Laboratory, USA) were used in this study also. All procedures were performed in accordance with guidelines for the care and use of laboratory animals at Yonsei University, as approved by the Association for Assessment and Accreditation of Laboratory Animal Care (AAALAC). Mice were anesthetized with 2.0% isoflurane under 30% oxygen and 70% nitrous oxide using a vaporizer (VMC Anesthesia Machine, MDS matrix; Orchard Park, NY, USA). Rectal temperature was controlled at 37 ± 0.5℃ with a

homeothermic blanket. For the sustained chronic administration of 3-NP mice model, 3-NP (Sigma, Milwaukee, WI, USA) was dissolved in saline to a concentration of 0.5 mg per μl (pH 7.4). The prepared solution of 3-NP was delivered by sustained infusion (180~190 mg/Kg/day) using osmotic minipumps at an infusion rate of 0.5 μl/h for seven days (1007D; Alzet, Cupertino, CA, USA). Mice infused with 3-NP were examined the degenerated brain region was validated with cresyl violet staining, and magnetic resonance image (MRI) analysis. For MRI analysis, we performed MRI scans of mice on a horizontal bore (400 mm) 4.7 Teslar MR scanner (Brucker Biospin, Billerica, MA, USA) after mice were anesthetized with isoflorane. Images were obtained using a T2-weighted fast spin echo sequence. Diffusion images were also acquired. Temperature was maintained and respiration was monitored throughout the entire scan. Mice recovered quickly following the scan with a 100% survival rate.

3. Behavior and motor function test

The motor functions of the mice were tested with the hindlimb clasping function. Mice were suspended by their tail and checked whether their hindlimb were clasped or not. The accelerating rotarod was performed on a rotarod apparatus (Ugo Basile North America Inc., Schwenksville, PA, USA) with speeds that varied from 4 to 40 r.p.m. for a maximum of 5 min. Each mouse was pre-trained prior to the implantation of the osmotic pump filled with 3-NP or saline. The training session was followed by a 30 min rest period, after which mice were placed back on the rotarod for five trials of five minutes maximum at accelerating speeds.

4. PCR and realtime PCR

Total RNA was isolated from mice striatum and cortex. Isolated RNA was purified and its quality determined and quantified by spectrophotometric analysis at 260 nm and 280 nm (NonoDrop). Ribonucleic acid (1 μg of total RNA) was reverse transcribed and cDNA was synthesized using PCR. The sequences of the forward and reverse BDNF primers are 5'-CGT GGG GAG CTG AGC GTG TGT-3' and 5'-GCC CCT GCA GCC TTC CTT CGT-3', respectively. A polymerase chain reaction (PCR) was performed as follows: initial denaturation at 95°C for 10 min, amplification (30 cycles) for 30 sec at 95°C, 30 sec at 60°C, 30 sec at 72°C, and a final extension at 70°C for 10 min. Following electrophoresis, RT-PCR products were visualized with a UV illuminator on an agarose gel. Reverse transcribed cDNA was also used in real-time PCR for ASK1 and p53. Real-time PCR was performed using a StepOne Plus (Applied Biosystems) or LightCycler rapid thermal cycler system (Roche Diagnostics, Lewes, UK). Reactions were performed in a 20 μl volume with 2 μl cDNA, 0.5 μM primers and reagents included in the DNA Master SYBR Green I mix (Roche Diagnostics). The forward (F) and reverse (R) primers used in the present study were shown in Table 1, which the primers for each target gene were designed by PrimerExpress 3.0 (Applied Biosystems). The reaction underwent pre-incubation step at 95℃ for 5 min, and was amplified by 45 cycles of denaturing at 95℃ for 15 sec and annealing and extending at 60℃ for 30sec. Detection of the fluorescent products was carried out at the end of the extension period. To assess an internal control GAPDH, house-keeping gene, mRNA was co-amplified in each sample. To confirm amplification specificity, the PCR was performed in no-transcript-control (NTC) and the PCR products from each primer pair were subjected to melting curve. For a melting curve analysis, the PCR products were melted by gradually increasing the temperature beginning at 65 ℃ in 0.2 ℃ steps. The

quantification data were analyzed with the ABI or LightCycler analysis software. Each sample was analyzed in triplicate to ensure the consistent results. Data analyzed by the comparative C*t* method. The $2^{-\Delta\Delta Ct}$ equation was used to determine quantitative comparison of the amplification of the each gene (Table 1). Each gene was analyzed in three biological replicates and three technical replicates. We used the average ΔCt from cortex or striatum. Data are presented as mean ± standard deviation (S.D.). Statistical evaluation of significant differences was performed using the Student's t-test. Differences of $p<0.05$ were considered statistically significant.

5. ATP assay

ATP level was evaluated by using ATP Colorimetric/Fluorometric Assay Kit (BioVision) and followed by manufacturer's procedures. Primary neurons (1×10^6 cells) or homogenized brain tissue (10 mg) were lysed ATP Assay Buffer. Each of samples was added to a 96-well plate and final volume was adjusted 50 ul with ATP Assay Buffer. For each well, reaction mix that is prepared with ATP assay buffer, ATP probe, and ATP converter was added 50ul into each well containing ATP standard and samples. After mixing well, plate was incubated at room temperature for 30 min under protection from light (or dark room). In micro-plate reader, absorbance (OD 570 nm) was measured, and ATP level of each sample were calculated by applying the standard curve.

6. Immunocytochemistry / immunohistochemistry and confocal microscopy

To determine the pattern of localization of each molecule, we performed immunofluorescent staining. After sacrificing the mice, the brains were remov ed, postfixed overnight in 3.7% formaldehyde, and stored in 30% sucrose. After fixation, the brains were cut into coronal sections of 20 μm thickness on a

cryostat section and processed for immunohistochemistry. Fixed sections were incubated with blocking solution as described previously [70] and incubated with a primary antibody at a dilution of 1:100. After washing, the sections were incubated with FITC-conjugated donkey anti-rabbit antibody (1:200; Jackson ImmunoResearch, West Grove, PA, USA). For counter-staining, the sections were incubated with DAPI or Hoechst 333342 (Molecular Probe). After washing, stained tissue samples were mounted using Vectashield mounting medium (Vector Lab, Burlingame, CA, USA). These sections were then obser ved under a confocal laser scanning microscope (Carl Zeiss, Thornwood, NY, USA). The sections were then cover-slipped and examined under a LSM510 confocal laser scanning microscope (Carl Zeiss).

7. Cell death assay

Caspase-3 activity, apoptosis-related DNA fragmentation, and TUNEL assay were evaluated using a commercial enzyme immunoassay kit (Chemicon International, Temecula, CA, USA) and a cytoplasmic histone-associated DNA fragment kit (Roche Diagnostics), and in situ Cell Death detection kit (Roche Diagnostics) respectively. According to manufacturer instructions, cytosolic samples (20 μg of protein) were used in each assay. Caspase-3 activity was determined to measure the quantity of bioluminescent substrate, DEVD-AFC, cleaved specifically by active caspase-3 as followed by manufacturer's protocol (EMD Bioscience, Darmstadt, Germany). In addition, we performed a TUNEL assay to detect cell death following the manufacturer's protocol (Roche Diagnostics)**.** Tissue were prepared as described above, and immune-fluorescent labeling was performed as previously described[40,41]. The sections were incubated with 50 ul of the TUNEL reaction mixture, and the sections were counterstained with Hoechst 333342 (Molecular Probe, USA), mounted, and

observed under a confocal laser scanning microscope (Carl Zeiss). The number of TUNEL-positive cells was counted in the striatum in three sections from each mouse at different levels.

8. ROS detection by in situ HEt and AP sites counting

For in situ detection of oxidized Het (Molecular Probes, Eugene, OR, USA), HEt (stock solution 100 mg/ml in dimethyl sulfoxide), which is oxidized to ethidium by superoxide anion radicals, was administered intravenously through the jugular vein 1 h after KA or saline injection (200 μl, 1 mg/ml). The brain sections were incubated with Hoechst 33258 (2.5×10−3 mg/ml; Molecular Probes) and fluorescence was assessed microscopically at an excitation of 510–550 nm and emission 580 nm for ethidium detection. The intensity and expression pattern of the oxidized HEt were observed using image analysis software (Metamorph ver4.6, Molecular Devices, Sunnyvale, CA, USA). To semiquantify ROS production, cells with oxidized HEt in the cytosol were counted and averaged in the entire field after random determination of four different areas, and the percentage of these cells to the total cells stained with Hoechst was calculated.

To measure the oxidative DNA damage, apurinic/apyrimidic sites arisen by ROS were counted. The isolated genomic DNA was subjected to quantitative analysis of AP sites using a colorimetric assay, following the manufacturer's protocol (Dojindo Molecular Technologies, Gaithersburg, MD, USA). Purified DNA was dissolved at a concentration of 100 μg/ml in TE and 10 μl of DNA solution was incubated with aldehyde reactive probe (ARP) solution. ARP in labeled DNA was measured using an ELISA-like assay in a microtiter plate. The number of AP sites per 10^5 nucleotides was calculated based on the linear calibration curve generated for each experiment using ARP-DNA standard

solutions.

9. Detection of DNA oxidation in mouse striatum

We evaluated DNA oxidation usinga monoclonal antibody against 8-OHdG according to a previous report [32]. The brain tissue was fixed, and treated with DNase-free RNase (Roche) at 37℃ for 1 h. Next, the sections were denatured in 4N HCl and neutralized with 50 mM Tris-base. After washing, the samples were incubated with an anti-mouse 8-OHdG antibody and also incubated with secondary antibody (MOM kit, Vector Laboratory, USA). The slides were mounted with Vectashield and coverslipped.

10. RNA interference (gene silencing with siRNA)

The ASK1 gene was silenced using siRNA against ASK1 (sense, GCUCGUAAUUUAUACACUGtt; antisense, CAGUGUAUAAAUUACGAGCtt; conc: 5 μM; Ambion, Austin, TX, USA). The silencing efficiency was confirmed in PC12 culture cells. After confirmation *in vitro*, the transfecting reagent, SiPORT *Neo*FX (Ambion), and ASK1-siRNA or nonfunctional mutant RNA (control siRNA, 5'-AAG AGA AAA AGC GAA GAG CCA-3'; Ambion) were combined, mixed gently, and allowed to form siRNA liposomes for an additional 10 min at room temperature. A micro-osmotic pump (Alzet), containing 100 μl of the transfection reagent only or ASK1-siRNA was then placed subcutaneously on the backs of the mice and a brain infusion cannula connected to a pump was positioned at the intra-striatum (anterior, 0.7 mm; lateral, 1.2 mm; depth, -3.3 mm) and also at the intra-cortex (anterior, 0.7 mm; lateral, -1.0 mm; depth, -2.0 mm). The designated solution was infused for seven days at a rate of 0.5 μL/h during 3-NP infusion. The mice were killed seven days after surgery and their brains were

processed. . In case of primary neuron, siRNA was treated at 12 days *in vitro* (DIV) and incubated for 72 hours with media change and the neuronal cell were additional treated and collected at 15 DIV.

11. Astrocyte conditioned medium

To test the effect of astrocyte derived unknown factor on neuron, we used astrocyte (C8-D1A) which was purchased from American Type Culture Collection (ATCC, Manassas, VA, USA). Astrocytes were cultured in Dulbecco's Modified Eagle's Medium high glucose (DMEM, Invitrogen, Carlsbad, CA, USA) supplemented with 10% fetal bovine serum (FBS, Invitrogen, USA) and 1% penicillin-streptomycin solution (Thermo Scientific, Waltham, MA, USA).The cultures were maintained at 37℃ in a humidified CO_2 incubator. For obtaining astrocyte conditioned medium (ACM), confluent astrocyte cell cultures were washed and replaced with serum-free medium DMEM/F12 (Thermo Scientific, USA) without FBS (Invitrogen, USA). Astrocytes in serum-free media were treated with 1mM 3-NP and incubated another 4 hours and 24 hours each. After then, media were collected and removed cell debris by centrifuging at 1,000*g* × 10 min. To evaluate the effect of ACM on neurons, primary neurons were cultured in Neurobasal media (NB, Invitrogen, USA). At 15 DIV, neurons were replaced the neurobasal media with ACM exposed to 3-NP and incubated additionally 4 hours. Effects of ACM on neuron were assessed by neuronal dendrites changes and immunocytochemistry of PSD95.

To further evaluate whether TGF-β1 of ACM mainly affected on neuronal dendrite degeneration and synaptic dysfunction, ACM was incubate with 1μg/mL TGF-β1 antibody (Abcam, Cambridge, MA, USA) for 30 min at room temperature to deplete TGF-β1 from ACM by neutralizing the TGF-β1. ACM

neutralizing TGF-β1 was also treated on neuron for 4 hours and neuronal changes were observed with dendritic morphologies and immunocytochemistry of PSD95. According to the manufacturer's information, TGF-β1 is neutralized 50% of the bioactivity when 0.25μg/mL TGF-β1 antibody was treated in HT2 cell line.

12. ELISA

The samples for ELISA were prepared in animal peripheral blood serum and ACM. Each ACM exposed to 3-NP for 4 hours and 24 hours each was collected and concentrated. Prepared ACM was performed according to the manufacturer's provided protocol. Standards were diluted with each assay buffer provided. Each assay was followed with each procedure. Plates were read and data were acquired. ELISA kits were obtained for total TGF-β1 (BioLegend, San Diego, CA, USA) and mouse C1q (Hycult Biotech, Uden, Netherlands).

13. Statistical analysis

Data are expressed as mean ± SD. The significance of differences among multiple groups was evaluated by ANOVA followed by Fisher's *post hoc* protected least-significant difference test, while two groups were compared using unpaired *t* tests (StatView, version 5.01; SAS Institute Inc, Cary, NC).

III. RESULTS

1. Selective striatal lesions were formed by systemic infusion of 3-NP in mice

Histological evaluation of the 3-NP-infused mice (n = 11 per time point) from day five demonstrated striatal abnormalities and scanty striatal lesions at day three (Figure 1A). We validated the lesion of mice infused by 3-NP using cresyl violet staining and the motor function test (Figure 1). Additionally DARPP32 (dopamine- and cyclic adenosine monophosphate-regulated phosphoprotein), an established of striatal neuron marker, showed weak immunoreactivity in 3-NP-infused mice (Figure 1). With motor function test, neurological and behavioral deficit were observed whether they showed hindlimb clasping, hindlimb dystonia and kyphotic posture, and whether they can adjust to a imbalanced postural challenges. Mice infused 3-NP were not displayed neurological deficit until day three (data not shown). In contrast, five days later, mice apparently showed hindlimb clasping (Figure 2) as well as hindlimb dystonia, kyphotic posture, and failure of imbalance adjustments (data not shown). Motor dysfunction was also evaluated at day three and seven following 3-NP infusion. Motor symptoms were prominent at day three and had worsened by day seven. The majority of 3-NP animal models could not remain on the rotarod (Figure 2, n = 12 each). It was determined to getting body weight loss along with the days after systemic 3-NP administration. The body weight fell down to 70% of initial body. At 7 days after 3-NP administration, the most of mice were presented the obvious symptoms like as weight loss and severe motor dysfunction, and consequently striatal lesion was formed in the mice.

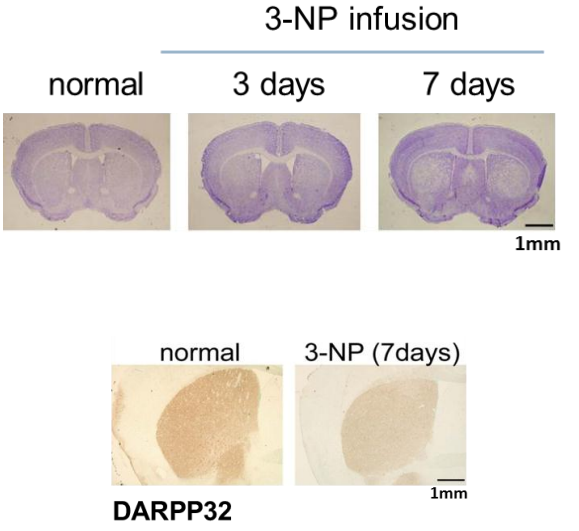

Figure 1. Chronic infusion of 3-NP induces selective striatal lesion. Cresyl violet staining demonstrates selective striatal cell loss at day seven. Corresponding to the result of cresyl violet staining, striatal neuron stained by DARPP32 were almost disappeared.

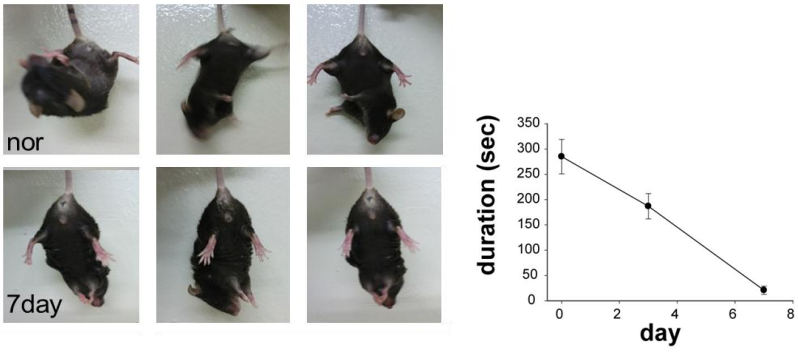

Figure 2. Chronic infusion of 3-NP induces behavioral and motor dysfunction. At day seven, the mice got hindlimb impaired. On the rotarod, they could not perform the rotarod test besides were hard to move. *p<0.05.

2. Mitochondrial dysfunction was triggered and ROS level was raised by 3-NP infusion

ATP measurements following infusion of 3-NP presented significant decreases in ATP content, according to 3-NP infused duration. At days three when the lesion was not detected, ATP level was sustained similar to the normal level (Figure 3A). However, for 7 days infused with 3-NP produced a 40% decrease in ATP levels (Figure 3A). The observed 40% reduction in ATP levels caused by application of 3-NP represents a significant decrement in neuronal metabolic capacity. Brain tissue and neurons exposed to 3-NP in this manner appeared morphologically normal, both initially and 3~4 days after the systemic exposure of insult. After 3–NP infusion, ROS production and oxidative DNA damage were detected by hydroethidine (HEt) oxidation, augmented AP sites number and the 8-hydroxy-2'-deoxyguanosine (8-OHdG)-positive cells by immunohistochemistry respectively. Oxidized Het by ROS are visible as small red particles. In contrast of red particles scantly shown in the normal tissue, a plenty of oxidized Het shown as red particles were displayed in the 3-NP infused tissue (Figure 3B). By infusion of 3-NP, oxidized HEt were increased and distributed in the striatum as well as cortex. Additionally apurinic/apyrimidic (AP) sites arisen by ROS were augmented from 3-NP infusion and the number of AP sites reached to summit at day seven (Figure 3C). Oxidative DNA damages triggered by 3-NP infusion were also examined with 8-OHdG immunohistochemistry, and there were detected plenty of 8-OHdG-positive cells both in the injured cortex and striatum corresponding to the result of HEt and AP sites number (Figure 3D). Representing DNA oxidation, 8-OHdG-positive cells were plenty in the 3-NP-infused striatum, and its immune-reactivity was strong in striatum. It suggests that the ROS was produced following mitochondrial dysfunction and subsequent DNA damage

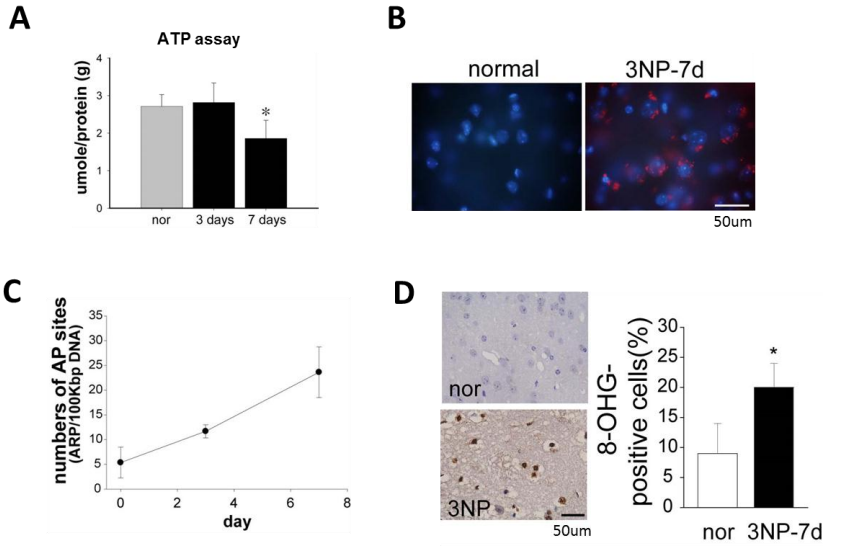

Figure 3. Infusion of 3-NP increases mitochondrial dysfunction and DNA damage. (A) ATP level decreased at day 7. (**B)** Hydroethidine bound with ROS is shown in red dots. (**C)** AP sites derived by overproducing ROS increased by day-dependent manner. (**D)** Another oxidative damage marker, 8-OHdG-positive cells also demonstrate oxidative damage by 3-NP infusion. **p*<0.05.

3. Brain-damage and apoptotic cell death were induced in the lesion of 3-NP infusion

The longer period of 3-NP infusion sustained, the greater amount of neuronal apoptotic cell death was occurred. The event impacted the cortex more than the striatum (Figure 4). The induction of DNA damage in striatal neurons was evaluated by terminal TUNEL staining (Figure 4). At day seven, the average number of TUNEL-positive nuclei was determined using multiple images in the four different mice of each group. These results demonstrate a statistically significant increase in TUNEL-positive nuclei in the 3-NP-infused mice, which was corresponded to the result of the DARPP32-positive cells in Figure 1. Caspase-3 and caspase-6 as the main effector of apoptotic cell death were evaluated the protein level with western blot analysis and also measured the activity with colorimetric analysis. It was demonstrated that caspase-6 was greatly higher in the striatum of 3-NP infused mice whereas caspase-3activity of 3-NP mice striatum was not much higher than the difference in caspase-6same different activity even after 3-NP chronic administration (Figure 4).

To evaluate the primary response protein amendment, both of ASK1 and p53 protein were analyzed by western blot assays (Figure 4 and 5); ASK1 was regarded as the initial responder to ROS, and p53 to DNA damage generated by 3-NP infusion each. The results revealed that the amounts of ASK1 and p53 protein were greater in 3-NP-infused mice than in vehicle-infused mice, and pASK1 (Thr845) was dominantly present at higher levels in the cortex than the striatum of 3-NP-infused mice (Figure 4). Levels of pASK1 (Thr845) were elevated in the cortex of 3-NP-infused mice, and the quantified graphs represent normalizing values with ASKl protein amounts. In the other hand, it is demonstrated in the striatal region that BDNF distribution and amounts were apparently reduced in the striatum at day seven after 3-NP infusion (Figure 7).

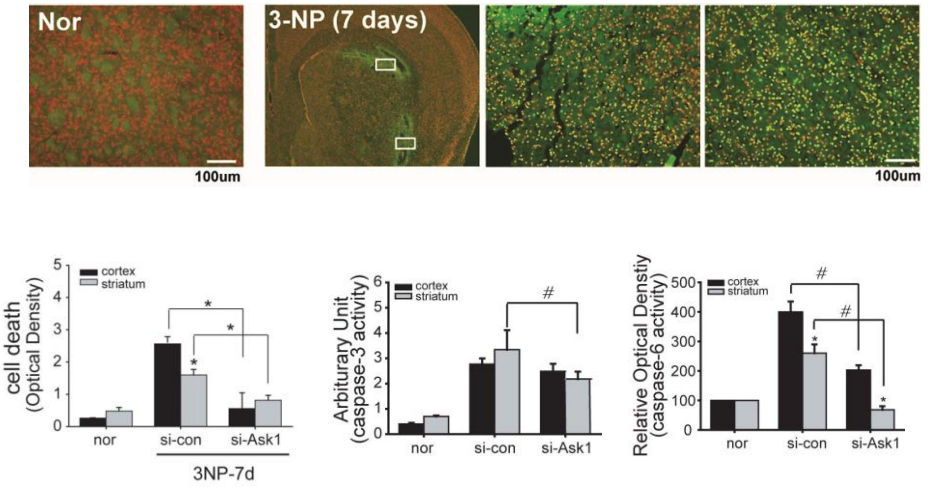

Figure 4. Apoptotic cell death was induced in the lesion of 3-NP infusion. At day seven, TUNEL-positive nuclei was detected mainly in the striatum especially lateral striatal region. Cell apoptotic cell death was assessed by cell death detection assay with cell lysates. Caspase-3 and caspase-6 were measured the activity with colorimetric analysis.

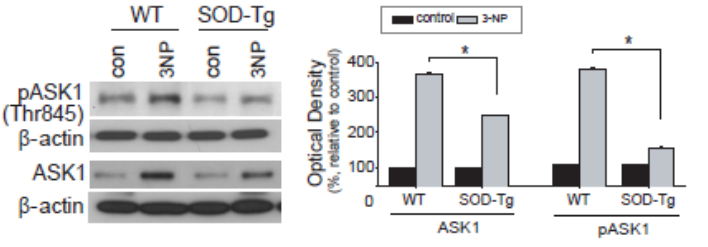

Figure 5. ASK1 protein level and activation were induced in the lesion of 3-NP infusion. The amounts of ASK1 protein were greater in 3-NP-infused mice than in vehicle-infused mice, and pASK1 (Thr845) was at higher levels in the cortex than the striatum of 3-NP-infused mice. Levels of pASK1 (Thr845) were significantly elevated in the cortex of 3-NP-infused mice, and the quantified graphs represent normalizing values with ASKl protein amounts.

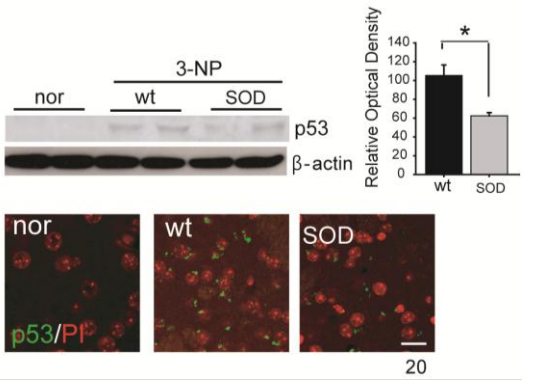

Figure 6. Protein level of p53 increased in the lesion of 3-NP infusion. DNA damage generated by 3-NP infusion triggered p53. The amounts of p53 protein were greater in 3-NP-infused mice than in vehicle-infused mice. Immunohisochemistry of p53 demonstrated in the striatal region that p53-postitive cells were more detected in the wt than SOD1 tg and distributed in nucleus at day seven after 3-NP infusion.

Scale bar = 20 μm; *$p < 0.01$

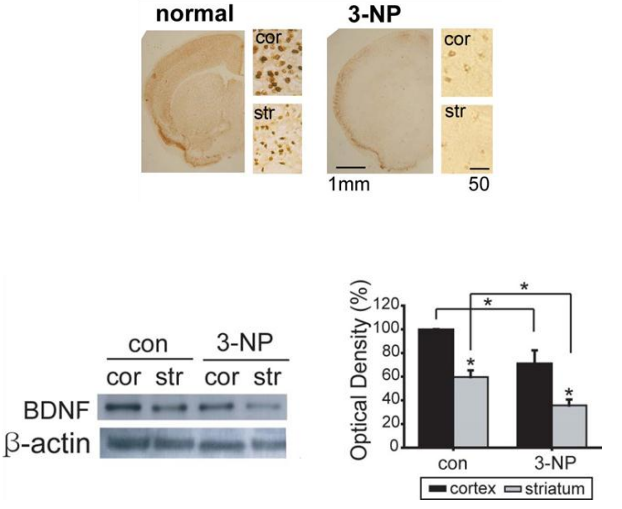

Figure 7. Infusion of 3-NP decreases BDNF expression. Immunohistochemisty showed that BDNF was almost depleted in striatum and cortex at day 7. Western blot analysis was also demonstrated the same results. *p<0.05.

4. Downregulation of ASK1 prevented 3-NP induced cell death, BDNF depletion, and subsequently improved the neurologic impairment

Decreases in BDNF protein levels in the cortical and striatal regions were apparently inhibited in siRNA-ASK1 treated 3-NP mice as compared to siRNA-control treated 3-NP infusion mice (Figure 8, n = 6 each). In IHC and western blot analysis of BDNF, the BDNF-positive cells were barely detected in the 3-NP infused cortex and striatum of the siRNA-control, whereas BDNF-positive cells increased as a result of BDNF restoration, particularly in the striatum of siRNA-ASK1 treated mice (Figure 8). In ASK1 gene-silenced mice, protein levels of BDNF were significantly higher whereas BDNF transcript levels were also restored in the cortex (Figure 8, n = 6 each). This result suggests that the inhibition of ASK1 blocks depletion of BDNF protein in the cortex and supply of BDNF protein into the striatum. ASK1 silencing not only resulted in increased levels of BDNF protein, but also in the significant recovery of BDNF mRNA levels in 3-NP injured and ASK1 gene silenced 3-NP infusion mice.

In vivo MRIs of siRNA-ASK1 treated 3-NP infusion mice were performed after the infusion of 3-NP and siRNA on day seven. In the contralateral side of the mice brain, progressive enlargement was evident in the lateral ventricles and atrophy was detected in the striatum. In the ipsilateral side, siRNA-ASK1 treated side, ventricular enlargement and striatal atrophy did not indicate severe regression (Figure 9, n = 4 each).

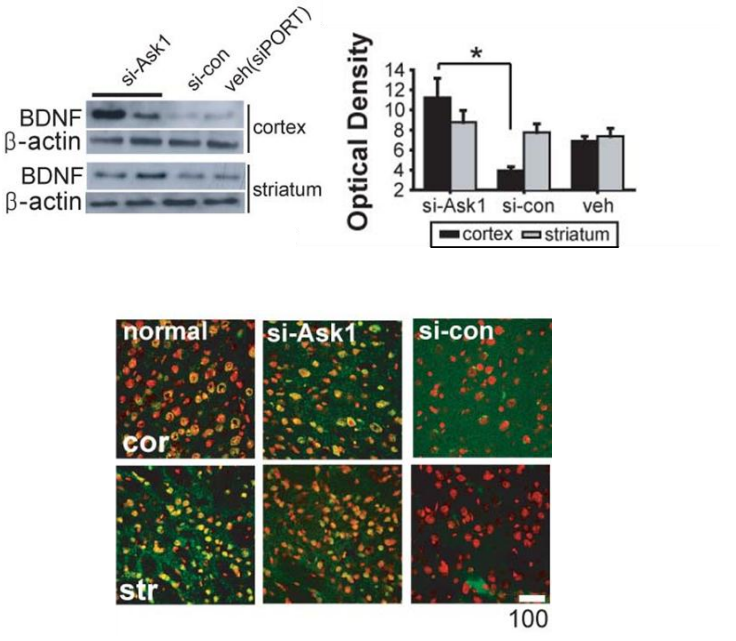

Figure 8. Down-regulating ASK1 prevents 3-NP induced BDNF depletion. BDNF amounts in cortex and striatum. Decreases of BDNF protein were prevented in ASK1-siRNA treated 3-NP mice compared to control-siRNA group. The immunohistochemistry of BDNF was also responsive to WB. The BDNF-positive cells were barely detected in control-siRNA group, whereas BDNF-positive cells were detected much more in ASK1-siRNA treated mice. Scale bar = 100 μm; cor, cortex; str, striatum; *$p < 0.01$

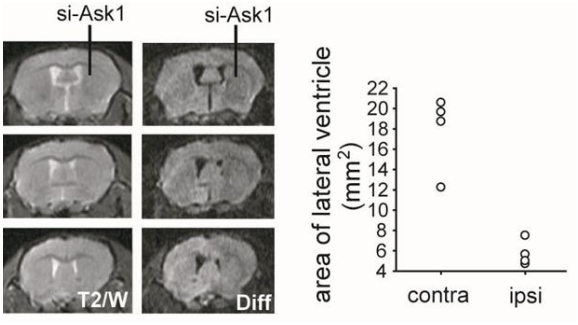

Figure 9. Down-regulation of ASK1 reduced striatal lesion size by 3-NP. MR images are demonstrated that the lateral ventricles in the contralateral side were enlarged and striatal atrophy was progressed. In the ipsilateral side, ASK1-siRNA treated side, ventricular enlargement and striatal atrophy were not indicated.

5. Infusion of 3-NP leads to striatum-selective astrocyte reactivation and changes the distribution of secreted BDNF, TGF-β1, and C1q protein in the damaged subregions

Neurons, stained with NeuN, homogeneously displayed in the cortex and striatum of control animals (Figure 10, left pannel), while neuronal staining was hardly found in the striatum of 3-NP infused mouse brain. Moreover, the neuronal loss was much more severe in striatum than in the cortex after 3-NP infusion for 7 days. Astrocytes were also weakly detected along the cortex and striatum of control rats (Figure 10, right pannel). In 3-NP infused mouse brain, GFAP immunostaining showed that astrocytes were strongly reactivated in the lateral striatum. However, distribution of reactivated astrocytes was not the whole striatum or cortex but lateral striatum where is the boundary between striatum and cortex. This result could be a hint that astrocyte related secreting molecule might be involved in selective striatal lesion formation followed by neuronal factors to impose neuronal loss or degeneration. Considering astrocyte derived molecules could involve in the neuronal loss, TGF-ß and C1q secretion level was assayed (Figure 11). The secretion levels of two molecules increased at day 3 when the lesion is not detected and also at day 7 when the lesion was definite. In addition, when the ASK1 is down-regulated, both of TGF-beta and C1q decreased their secretion level. After 3-NP infusion, TGF-β1 was highly secreted at 3 days when it is the time before lesion formation. At 7 days when the specific striatal lesion was fully and completely developed, TGF-β1 level was reduced rather than that at 3 days (Figure 11). C1q secretion level was also corresponding to the level of TGF-β1 (Figure 11).

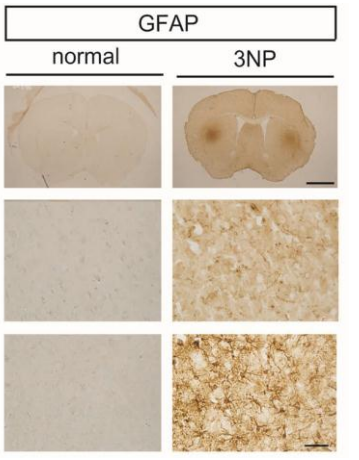

Figure 10. Astrocytes were strongly reactivated by infusion of 3-NP. Astrocytes reactivated selectively in the lateral striatum.

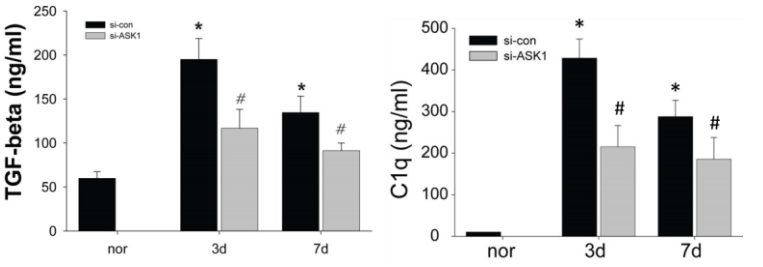

Figure 11. TGF-beta and C1q secretion was triggered by 3-NP infusion. The secretion level of TGF-β1 and C1q evaluated by ELISA. The secretion levels of two molecules increased at day 3 when the lesion is not detected and also at day 7 when the lesion was definite. In addition, when the ASK1 is down-regulated, both of TGF-β1 and C1q decreased their secretion level.

6. TGF-β1 is differentially expressed in the damaged brain subregions and astrocyte derived ASK 1 by 3-NP involves in TGF- β1

TGF-β1 mRNA expression evaluated using RT-PCR was different in various brain regions of 3-NP-induced mice (Figure 12, upper). The alteration of TGF-β1 in the cortex and striatum were assessed in the brains of 3-NP infused mice (Figure 12, upper). Corresponding to the result of TGF-β1 ELISA in the whole blood serum, more TGF-β1 transcripts were present in the striatum than in the cortex of 3-NP-infused mice. It showed that TGF-β1 differentially expressed in brain subregions by days after 3-NP infusion. TGF-β1 transcript highly increased in striatum while cortical TGF-β1 transcript was not shown the significance. To test that the expression level of TGF-β1 is affected by ASK1 level, we down-regulated the ASK1 level with siRNA-ASK1 into striatlal region. Down-regulating ASK1, however, did not lower TGF-β1 transcript in striatum either cortex. Nevertheless, down-regulating ASK1 showed neuroprotective effect in striatal neuron stained with NeuN (Figure 12, lower). To further evaluate the effect of TGF-β1 on neuron, we used astrocyte cells exposing to 1mM 3-NP for chronic and mild intoxication. Exposure of 3-NP onto astrocyte increased TGF-β1 expression level and ASK1 protein amounts (Figure 13). As same in the above results of animal, down-regulating ASK1 had no effect to reduce astrocyte TGF-β1 transcription level (Figure 13).

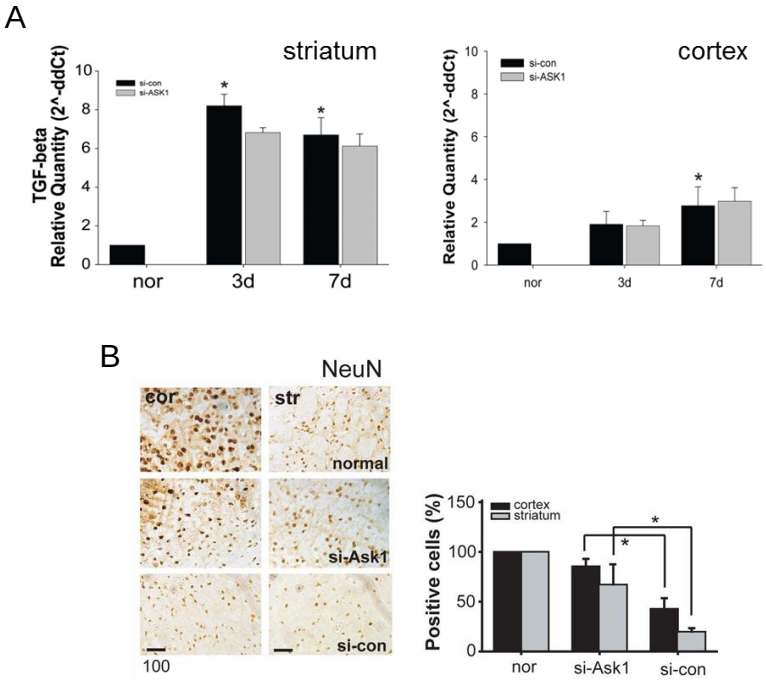

Figure 12. TGF-beta is differentially expressed in brain subregions and astrocyte derived ASK 1 by 3-NP involves in TGF- β1. (A) Realtime RT-PCR of TGF-β1 in cortex and striatum. TGF-β1 transcript highly increased in striatum while cortical TGF-β1 transcript was not shown the significance. Down-regulating ASK1 did not lower TGF-β1 transcript. **(B)** Immunohistochemistry of NeuN in each cortex and striatum. Although down-regulated ASK1 did not alter the transcriptional level of TGF-β1, down-regulating ASK1 showed neuroprotective effect in striatal neuron.

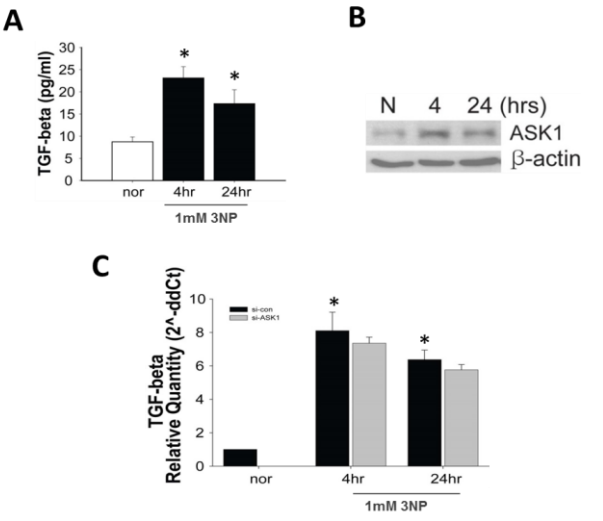

Figure 13. Infusion of 3-NP alters TGF- β1 and ASK1 in astrocyte. Astrocytes were cultured and exposed to 1mM 3-NP for chronic and mild intoxication. (**A)** The secreted TGF-β1 was augmented and (**B)** also ASK1 protein level of astrocyte increased by 3-NP treatment. (**C)** Down-regulating ASK1 did not reduce astrocyte TGF-β1 transcript.

7. TGF-β1 secreted by astrocyte triggers neuronal C1q degenerating neuronal dendrites and ASK1 mediates the event

To evaluate whether astrocyte conditioned media (ACM) containing TGF-β1 can affect neuron cytotoxicity, we used primary neuron culture. As same in the case of astrocyte culture, neuronal cells were exposed to 1mM 3-NP for chronic and mild intoxication. The ATP level is similar pattern to that of animal model (Figure 14A). Specifically for assessing the regulating role of astrocyte on neuron, ACM was prepared to expose to 3-NP for 4 hours and 24hours each. Neuron was replaced by prepared ACM and then incubated for another 4 hours. The qPCR results demonstrated that neuronal C1q transcript was highly expressed under ACM (Figure 14B). When ASK1 and C1q were down-regulated in neuron, however, neuronal C1q transcript decreased even if under ACM containing TGF-β1. When neuronal media were replaced by ACM, although neuronal cell death was not detected, there were some changes in the neuronal dendrites by immunostaining with PSD95 (Figure 14C). Under condition of augmented astrocyte TGF-β1 in 3-NP infused animal, C1q secretion level increased as mentioned above that ASK1 expression level was linked with C1q and followed by change of ASK1 expression level (Figure 11) After 3-NP infusion, C1qR-positive cells were detected more in ASK1 downregulated striatum (Figure 15). We assumed that changed C1q level could bring the striatal cell loss. To certify the assumption, we applied C1q directly into the striatum and cortex each and examined whether neuronal cell demise can be caused by C1q or not. As shown in Figure 15, lots of TUNEL-positive cells were in striatum contrast to cortex, even though the same dose of C1q (Figure 15).

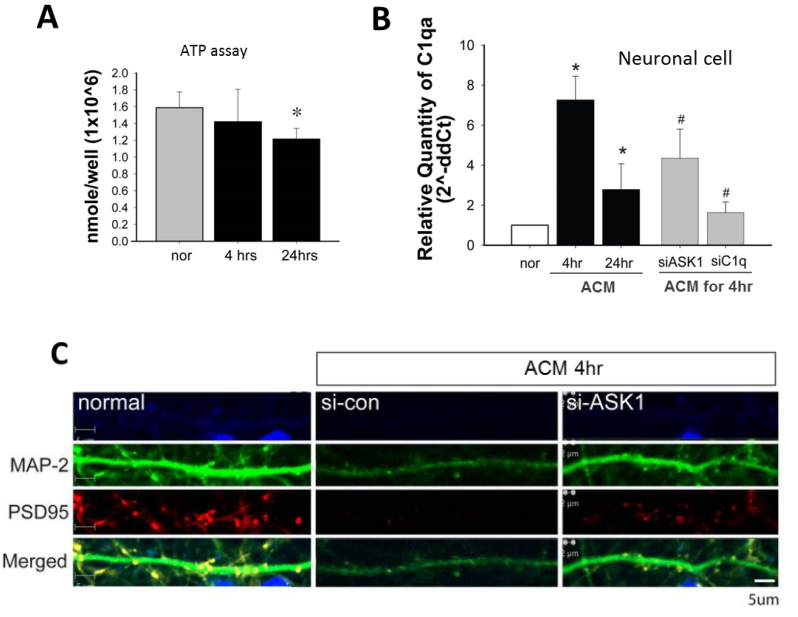

Figure 14. Astrocyte conditioned media (ACM) affect on neuron to trigger neuronal C1q degenerating neuronal dendrites and ASK1 mediates the event. (**A)** The ATP level is lowered at 24 hours after exposure to 1mM 3-NP. (**B)** Astrocytes were exposed to 3NP for 4 hours and 24 hours each. Neuron was replaced by prepared ACM and then incubated for another 4 hours. Neuronal C1q transcript is highly expressed under ACM. When ASK1 and C1q were down-regulated in neuron, however, neuronal C1q transcript decreased even if under ACM. (**C)** When neuronal media were replaced by ACM, although neuronal cells were not died, there were some changes in the neuronal dendrites.

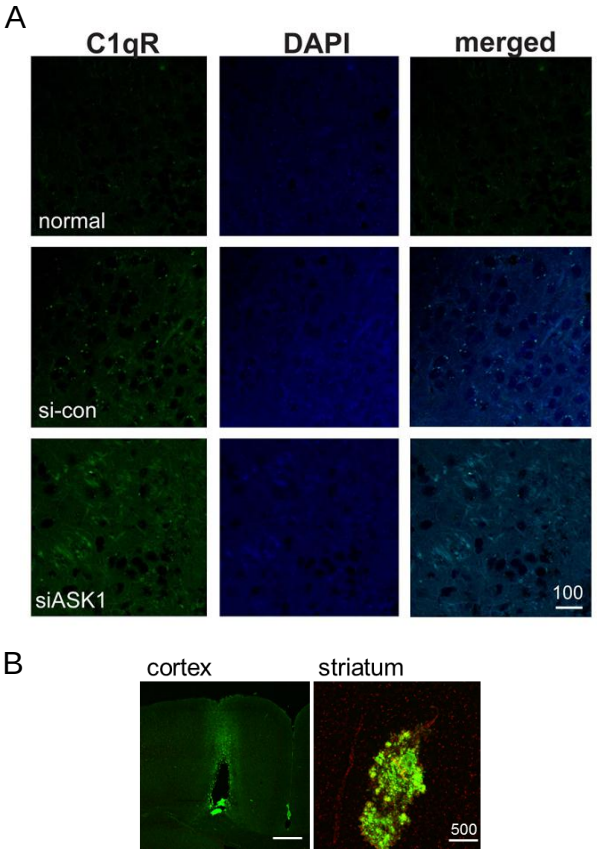

Figure 15. Infusion of 3-NP increases C1qR mediated by ASK1. (A) At five days after 3-NP infusion, C1qR-positive cells were detected more in ASK1 downregulated striatum. According to increased C1q secretion level, C1qR-positive signals were detected in the striatal damaged lesion. Down-regulating ASK1 reduced the C1qR-postive signals despite of 3-NP infusion. **(B)** When C1q directly injected into the striatum and cortex each, lots of TUNEL-positive cells were in striatum contrast to cortex, even though the same dose of C1q.

IV. DISCUSSION

The results of the present work show an improvement in behavioral impairment by ASK1 down-regulation, despite 3-NP infusion. We propose the hypothesis that (1) ASK1 overexpression by systemic infusion of 3-NP promotes the formation of selective striatal lesions, and this occurs apart from just ROS generation. (2) ASK1 may differentially regulate C1q secretion level via active TGF-beta in each brain subregion of cortex and striatum, consequently involved in axon degeneration of corticostriatal projection neuron. When brain is mildly and chronically exposed to mitochondrial toxin, presynaptic neuron (in cortical neuron) degrades first, and then postsynaptic neuron of striatal MSN neuron withers as a consequence of it. We suppose that striatal lesion formation results from the non-autonomous events as hypothesis described above.

The systemic administration of 3-NP causes selective degeneration of neurons in the lateral striatum, few reports have infused 3-NP into mice using a subcutaneous osmotic pump, which differs from previous studies on rats [4,28,71]. HD is caused by a dominant inherited expansion of CAG repeats in the Huntington gene. Thus, many aspects of HD cannot be mimicked by 3-NP. However, recent research shows that mitochondrial defects and oxidative stress may play a key role in HD pathogenesis, further supporting the potential utility of the 3-NP model of striatal degeneration [72]. Our results demonstrated that the systemic infusion of 3-NP into mice caused selective striatal lesions, apparent motor dysfunction, and cell death by day seven (Figure 1). The 3-NP infusion mice model was used in this study because a treatment could be concomitantly added at the beginning of pathogenesis. By treating the siRNA-ASK1 with 3-NP infusion, this provided a chance to examine selective striatal vulnerability

resulting from systemic 3-NP administration. chronic systemic administration of 3-NP in rats and non-human primates produces homogeneous inhibition of complex II (SDH) within the brain and not solely the striatum [28,73], despite evident striatal degeneration associated with behavioural abnormalities that are reminiscent of HD [27,74]. In our study we were mainly interested in studying mild 3-NP neurotoxicity. We used 3-NP at a concentration that while decreasing SDH activity by approximately 75% did not affect the activity of the other mitochondrial complexes or ATP levels (Figure 3). Indeed, maintenance of cellular ATP levels is important for apoptotic cell death.

Mitochondria are key players in the production of ROS and have been reported to have an important role in 3-NP injury-induced pathology [42] and also oxidative DNA damage results from direct ROS attacks. There are some types of oxidative DNA damage detective method. Among them, 8-OHdG results in oxidative DNA damage. The results presented here show that the oxidative DNA lesions are markedly augmented in the 3-NP-infused wt mouse brain. Once ROS are generated, they can damage mitochondria causing additional free-radical generation and loss of antioxidant capacity, leading to a deleterious cycle [4]. Therapeutic prevention of oxidative stress has been proposed to "break the cycle" of cell death[4], and studies have been carried out in the neurodegenerative field attempting to modulate key enzymatic components that regulate oxidative stress [33]. Our study was performed on the assumption that mitochondrial complex II inhibitors generate ROS, and contribute to cell death. Furthermore, because ASK1is known to be involved in ROS-induced cell death, we propose that ASK1 plays an instrumental role and even amplifies this process. The ASK1 signaling-mediated cell fate decision appears to depend in part on the extent and duration of ASK1 amounts and its activation. A previous report found that a mutated SOD induced ER stress and activated the

ASK1-mediated cell death pathway [13]. Also, the deletion of ASK1 mitigated neuronal loss and extended the life span of SOD1-mutated mice [13]. Recent studies with animal models have revealed that oxidative stress is a causative factor in the initiation and progression of Alzheimer's disease (AD) and Parkinson's disease, where antioxidants have the capacity to attenuate the phenotypes associated with these neurodegenerative disorders. Although antioxidants can prevent the oxidative stress-mediated progression of neurodegenerative diseases [47], antioxidant treatment is not sufficient to halt disease progression. We implied that inhibition of ASK1, the major downstream activator, may disrupt the positive feedback Therefore we propose that mitochondrial dysfunction by 3-NP induces an increase in ROS level; ROS-activated ASK1 mediates harmful oxidative signals; and cells eventually undergo apoptosis. The precise mechanisms have not yet been elucidated and have to be investigated.

Because the majority of striatal BDNF is synthesized by cortical neurons, the data also imply that cortical dysfunction contributes to HD's hallmark effects on the basal ganglia [57]. Finally, the results suggest that striatal lesions caused by mitochondrial toxins may arise via pathways different from those that drive striatal neurodegeneration in 3-NP infused animal. According to the P35 expression profiles, the similar mRNA expression changes argue that the MSNs in HD and BDNF-deprived environments suffer from similar insults [57]. The 3-NP profile appears substantially attributable to astrocytosis, a common component of HD, but not HD-specific or necessarily a significant feature of early HD [75]. Through the study, reductions in striatum-enriched mRNAs associated with MSN dysfunction failed to appear although the 3-NP regimen has been optimized to produce striatal lesions. The result may indicate that 3-NP lesions arise via rapid apoptotic mechanisms [57]. BDNF is primarily supplied to

the striatum via anterograde transport down corticostriatal axons [76], which BDNF depletion in the striatum may be particularly sensitive to disrupted axonal transport [57]. In the current study, systemic 3-NP infusion was followed by BDNF protein decreased in cortical neurons (Figure 7). In case of HD, Colin et al. also reported that BDNF flow and release is increased via Htt phosphorylation [76]. Collectively in the previous reports, we observed that the BDNF protein levels primarily and abundantly increased in the cortex and then BDNF proteins were also restored the injured striatum after the siRNA-ASK1 treatment of 3-NP infused mice. Recent reports indicate that disturbance of BDNF transportation to the striatum results in striatal selectivity in 3-NP degeneration as opposed to toxicity of mHtt itself [5,22]. Patients later exhibit dystonia, which indicates the development of striatal lesions. Brain MRIs confirm this also [77]. These clinical findings strongly support an initial BDNF-transport disturbance induced by cerebral mHtt that may result in striatal vulnerability. Some reports elucidated the relationship between mHtt fragments and BDNF depletion as that endogenous intact Htt protein disappeared after 3-NP treatment in cultured cells, resulting in reduced BDNF protein levels [25,78]. Moreover, the restoration of depleted cortical BDNF facilitates successful HD treatment in the HD patients [79]. Recovery of BDNF by gene silencing of ASK1 led the striatal atrophy in the ipsilateral side infused siRNA to be ameliorated though MRI images, and eventually motor function to be improved (Figure 9). Our results imply that the selective elimination of ASK1 by siRNA as well as its activity inhibits caspase-6 activity and impedes striatal neurodegeneration *in vivo*. The gene silencing of ASK1 facilitates the restoration of cortical BDNF, which then increases the supply of BDNF protein in the striatum. BDNF is highly concentrated in the nervous system but is also found in the blood of human and other mammals, where its function is poorly understood [80]. Although

it is still unclear how BDNF expression and metabolism in human peripheral tissues are regulated, changes in serum BDNF levels in rats during development correlate with those in the brain [81]. Studies in rodents in which BDNF mRNA and protein have been evaluated both in basal conditions and after pharmacological treatment are promising [82,83]. In particular, the level of BDNF mRNA can be monitored systematically, and it correlates with disease progression in R6/2 mice and HD rats [84]. Blood BDNF mRNA is also sensitive to pharmacological treatments. It can be used to test compounds in HD mice, predict their ability to stimulate the production of BDNF in the brain, and possibly evaluate their therapeutic efficacy in the animals by a blood test. However, detection of BDNF in HD patients requires standardization in the collection and the processing methodology of a large number of samples

C1q, a complement factor deposited in classical innate immune pathway, has been reported to affect ROS and mediate neuronal injury during AD [85]. The study reported that the blocking of neuronal calreticulin by its antibody abrogated ROS by C1q, and suggested that the C1q may be an important factor contributing to neuronal oxidative stress and neuronal demise during AD [85]. In that TGF-β signaling, Serine-threonine kinase receptor-associated protein (STRAP) which is identified an interacting partner of ASK1was issued to interact with TGF-β receptors and block TGF-β signaling [86]. ASK1 phosphorylated STRAP, inhibition of ASK1 suppress the hydroxyl peroxide induced apoptosis mediating STRAP by directly interacting between ASK1 and STRAP. The regulatory role of ASK1 in C1q level may be consistent with this report that the ASK1 is working as a negative regulator of STRAP activating TGF-β signaling. Until now**,** the signals controlling C1q expression and function remain elusive. Previous report identified that retinal TGF-β play a key regulator role in of neuronal C1q expression and synaptic pruning in the

developing visual system [87]. C1q rapidly upregulated by TGF-β from astrocyte, and TGF-beta is essentially needed to that. Specific in retinal development and eye-segregation, controlling of C1q level by TGF-β is decisive [88]. GFAP-positive astrocytes are distributed in the neonatal brain with a similar regional heterogeneity. Although the GFAP-positive astrocytes showed in different pattern during the developmental period, and did not disappear in the regional differential pattern at the stage of postnatal, regional allocation of reactive astrocyte may be induced by injury.

V. CONCLUSION

Consolidating these results, we posit an interpretation for selective striatal vulnerability against systemic 3-NP infusion. We suggest that the increased ASK1 is linked to regulation of TGF-β secreted in astrocytes, and differential C1q expression in neurons triggered by TGF-β1 leads degradation of cortical projection and depletion of BDNF in striatal neuron in mice brains systemically infused with 3-NP.

REFERENCES

1. Katayama T, Imaizumi K, Sato N, Miyoshi K, Kudo T, Hitomi J, et al. Presenilin-1 mutations downregulate the signalling pathway of the unfolded-protein response. Nat Cell Biol 1999;1:479-85.
2. Imai Y, Soda M, Inoue H, Hattori N, Mizuno Y, Takahashi R. An unfolded putative transmembrane polypeptide, which can lead to endoplasmic reticulum stress, is a substrate of Parkin. Cell 2001;105:891-902.
3. Nishitoh H, Matsuzawa A, Tobiume K, Saegusa K, Takeda K, Inoue K, et al. ASK1 is essential for endoplasmic reticulum stress-induced neuronal cell death triggered by expanded polyglutamine repeats. Genes Dev 2002;16:1345-55.
4. Lin MT, Beal MF. Mitochondrial dysfunction and oxidative stress in neurodegenerative diseases. Nature 2006;443:787-95.
5. Cattaneo E, Zuccato C, Tartari M. Normal huntingtin function: an alternative approach to Huntington's disease. Nat Rev Neurosci 2005;6:919-30.
6. Waelter S, Boeddrich A, Lurz R, Scherzinger E, Lueder G, Lehrach H, et al. Accumulation of mutant huntingtin fragments in aggresome-like inclusion bodies as a result of insufficient protein degradation. Mol Biol Cell 2001;12:1393-407.
7. Liu Y, Chang A. Heat shock response relieves ER stress. Embo J 2008;27:1049-59.
8. Bence NF, Sampat RM, Kopito RR. Impairment of the ubiquitin-proteasome system by protein aggregation. Science 2001;292:1552-5.

9. Warrick JM, Chan HY, Gray-Board GL, Chai Y, Paulson HL, Bonini NM. Suppression of polyglutamine-mediated neurodegeneration in Drosophila by the molecular chaperone HSP70. Nat Genet 1999;23:425-8.
10. Sekine Y, Takeda K, Ichijo H. The ASK1-MAP kinase signaling in ER stress and neurodegenerative diseases. Curr Mol Med 2006;6:87-97.
11. Luo D, He Y, Zhang H, Yu L, Chen H, Xu Z, et al. AIP1 is critical in transducing IRE1-mediated endoplasmic reticulum stress response. J Biol Chem 2008;283:11905-12.
12. Arning L, Monte D, Hansen W, Wieczorek S, Jagiello P, Akkad DA, et al. ASK1 and MAP2K6 as modifiers of age at onset in Huntington's disease. J Mol Med 2008;86:485-90.
13. Nishitoh H, Kadowaki H, Nagai A, Maruyama T, Yokota T, Fukutomi H, et al. ALS-linked mutant SOD1 induces ER stress- and ASK1-dependent motor neuron death by targeting Derlin-1. Genes Dev 2008;22:1451-64.
14. Minn Y, Cho KJ, Kim HW, Kim HJ, Suk SH, Lee BI, et al. Induction of apoptosis signal-regulating kinase 1 and oxidative stress mediate age-dependent vulnerability to 3-nitropropionic acid in the mouse striatum. Neurosci Lett 2008;430:142-6.
15. Lee BI, Lee DJ, Cho KJ, Kim GW. Early nuclear translocation of endonuclease G and subsequent DNA fragmentation after transient focal cerebral ischemia in mice. Neurosci Lett 2005;386:23-7.
16. Wang H, Yu SW, Koh DW, Lew J, Coombs C, Bowers W, et al. Apoptosis-inducing factor substitutes for caspase executioners in NMDA-triggered excitotoxic neuronal death. J Neurosci 2004;24:10963-73.

17. Chen ZL, Strickland S. Neuronal death in the hippocampus is promoted by plasmin-catalyzed degradation of laminin. Cell 1997;91:917-25.
18. Gu Z, Cui J, Brown S, Fridman R, Mobashery S, Strongin AY, et al. A highly specific inhibitor of matrix metalloproteinase-9 rescues laminin from proteolysis and neurons from apoptosis in transient focal cerebral ischemia. J Neurosci 2005;25:6401-8.
19. Peng Q, Masuda N, Jiang M, Li Q, Zhao M, Ross CA, et al. The antidepressant sertraline improves the phenotype, promotes neurogenesis and increases BDNF levels in the R6/2 Huntington's disease mouse model. Exp Neurol 2008;210:154-63.
20. Wellington CL, Ellerby LM, Gutekunst CA, Rogers D, Warby S, Graham RK, et al. Caspase cleavage of mutant huntingtin precedes neurodegeneration in Huntington's disease. J Neurosci 2002;22:7862-72.
21. Li H, Li SH, Johnston H, Shelbourne PF, Li XJ. Amino-terminal fragments of mutant huntingtin show selective accumulation in striatal neurons and synaptic toxicity. Nat Genet 2000;25:385-9.
22. Hermel E, Gafni J, Propp SS, Leavitt BR, Wellington CL, Young JE, et al. Specific caspase interactions and amplification are involved in selective neuronal vulnerability in Huntington's disease. Cell Death Differ 2004;11:424-38.
23. Chen C, Fuhrken PG, Huang LT, Apostolidis P, Wang M, Paredes CJ, et al. A systems-biology analysis of isogenic megakaryocytic and granulocytic cultures identifies new molecular components of megakaryocytic apoptosis. BMC Genomics 2007;8:384.
24. Shimoke K, Utsumi T, Kishi S, Nishimura M, Sasaya H, Kudo M, et al. Prevention of endoplasmic reticulum stress-induced cell death by

brain-derived neurotrophic factor in cultured cerebral cortical neurons. Brain Res 2004;1028:105-11.

25. Zuccato C, Ciammola A, Rigamonti D, Leavitt BR, Goffredo D, Conti L, et al. Loss of huntingtin-mediated BDNF gene transcription in Huntington's disease. Science 2001;293:493-8.

26. Gu X, Andre VM, Cepeda C, Li SH, Li XJ, Levine MS, et al. Pathological cell-cell interactions are necessary for striatal pathogenesis in a conditional mouse model of Huntington's disease. Mol Neurodegener 2007;2:8.

27. Beal MF, Brouillet E, Jenkins BG, Ferrante RJ, Kowall NW, Miller JM, et al. Neurochemical and histologic characterization of striatal excitotoxic lesions produced by the mitochondrial toxin 3-nitropropionic acid. J Neurosci 1993;13:4181-92.

28. Bizat N, Hermel JM, Boyer F, Jacquard C, Creminon C, Ouary S, et al. Calpain is a major cell death effector in selective striatal degeneration induced in vivo by 3-nitropropionate: implications for Huntington's disease. J Neurosci 2003;23:5020-30.

29. Lee WT, Yin HS, Shen YZ. The mechanisms of neuronal death produced by mitochondrial toxin 3-nitropropionic acid: the roles of N-methyl-D-aspartate glutamate receptors and mitochondrial calcium overload. Neuroscience 2002;112:707-16.

30. Almeida S, Laco M, Cunha-Oliveira T, Oliveira CR, Rego AC. BDNF regulates BIM expression levels in 3-nitropropionic acid-treated cortical neurons. Neurobiol Dis 2009;35:448-56.

31. Kumar P, Kalonia H, Kumar A. Cyclosporine A attenuates 3-nitropropionic acid-induced Huntington-like symptoms in rats: possible nitric oxide mechanism. Int J Toxicol 2010;29:318-25.

32. Kim GW, Chan PH. Oxidative stress and neuronal DNA fragmentation mediate age-dependent vulnerability to the mitochondrial toxin, 3-nitropropionic acid, in the mouse striatum. Neurobiol Dis 2001;8:114-26.
33. Andersen JK. Oxidative stress in neurodegeneration: cause or consequence? Nat Med 2004;10 Suppl:S18-25.
34. Hsu MJ, Hsu CY, Chen BC, Chen MC, Ou G, Lin CH. Apoptosis signal-regulating kinase 1 in amyloid beta peptide-induced cerebral endothelial cell apoptosis. J Neurosci 2007;27:5719-29.
35. Ichijo H, Nishida E, Irie K, ten Dijke P, Saitoh M, Moriguchi T, et al. Induction of apoptosis by ASK1, a mammalian MAPKKK that activates SAPK/JNK and p38 signaling pathways. Science 1997;275:90-4.
36. Saitoh M, Nishitoh H, Fujii M, Takeda K, Tobiume K, Sawada Y, et al. Mammalian thioredoxin is a direct inhibitor of apoptosis signal-regulating kinase (ASK) 1. Embo J 1998;17:2596-606.
37. Tobiume K, Matsuzawa A, Takahashi T, Nishitoh H, Morita K, Takeda K, et al. ASK1 is required for sustained activations of JNK/p38 MAP kinases and apoptosis. EMBO Rep 2001;2:222-8.
38. Fox JH, Barber DS, Singh B, Zucker B, Swindell MK, Norflus F, et al. Cystamine increases L-cysteine levels in Huntington's disease transgenic mouse brain and in a PC12 model of polyglutamine aggregation. J Neurochem 2004;91:413-22.
39. Cho KJ, Lee BI, Cheon SY, Kim HW, Kim HJ, Kim GW. Inhibition of apoptosis signal-regulating kinase 1 reduces endoplasmic reticulum stress and nuclear huntingtin fragments in a mouse model of Huntington disease. Neuroscience 2009.
40. Kim GW, Chan PH. Involvement of superoxide in excitotoxicity and

DNA fragmentation in striatal vulnerability in mice after treatment with the mitochondrial toxin, 3-nitropropionic acid. J Cereb Blood Flow Metab 2002;22:798-809.

41. Heo K, Cho YJ, Cho KJ, Kim HW, Kim HJ, Shin HY, et al. Minocycline inhibits caspase-dependent and -independent cell death pathways and is neuroprotective against hippocampal damage after treatment with kainic acid in mice. Neurosci Lett 2006;398:195-200.
42. Sawa A, Wiegand GW, Cooper J, Margolis RL, Sharp AH, Lawler JF, Jr., et al. Increased apoptosis of Huntington disease lymphoblasts associated with repeat length-dependent mitochondrial depolarization. Nat Med 1999;5:1194-8.
43. Dunah AW, Jeong H, Griffin A, Kim YM, Standaert DG, Hersch SM, et al. Sp1 and TAFII130 transcriptional activity disrupted in early Huntington's disease. Science 2002;296:2238-43.
44. Bucana C, Saiki I, Nayar R. Uptake and accumulation of the vital dye hydroethidine in neoplastic cells. J Histochem Cytochem 1986;34:1109-15.
45. Santamaria A, Perez-Severiano F, Rodriguez-Martinez E, Maldonado PD, Pedraza-Chaverri J, Rios C, et al. Comparative analysis of superoxide dismutase activity between acute pharmacological models and a transgenic mouse model of Huntington's disease. Neurochem Res 2001;26:419-24.
46. Kim GW, Gasche Y, Grzeschik S, Copin JC, Maier CM, Chan PH. Neurodegeneration in striatum induced by the mitochondrial toxin 3-nitropropionic acid: role of matrix metalloproteinase-9 in early blood-brain barrier disruption? J Neurosci 2003;23:8733-42.
47. Bahadorani S, Hilliker AJ. Antioxidants cannot suppress the lethal

phenotype of a Drosophila melanogaster model of Huntington's disease. Genome 2008;51:392-5.

48. Almeida S, Domingues A, Rodrigues L, Oliveira CR, Rego AC. FK506 prevents mitochondrial-dependent apoptotic cell death induced by 3-nitropropionic acid in rat primary cortical cultures. Neurobiol Dis 2004;17:435-44.

49. Wu CL, Hwang CS, Chen SD, Yin JH, Yang DI. Neuroprotective mechanisms of brain-derived neurotrophic factor against 3-nitropropionic acid toxicity: therapeutic implications for Huntington's disease. Ann N Y Acad Sci 2010;1201:8-12.

50. Brouillet E, Jenkins BG, Hyman BT, Ferrante RJ, Kowall NW, Srivastava R, et al. Age-dependent vulnerability of the striatum to the mitochondrial toxin 3-nitropropionic acid. J Neurochem 1993;60:356-9.

51. Gizatullina ZZ, Lindenberg KS, Harjes P, Chen Y, Kosinski CM, Landwehrmeyer BG, et al. Low stability of Huntington muscle mitochondria against Ca2+ in R6/2 mice. Ann Neurol 2006;59:407-11.

52. Browne SE. Mitochondria and Huntington's disease pathogenesis: insight from genetic and chemical models. Ann N Y Acad Sci 2008;1147:358-82.

53. Alam ZI, Halliwell B, Jenner P. No evidence for increased oxidative damage to lipids, proteins, or DNA in Huntington's disease. J Neurochem 2000;75:840-6.

54. Cho KJ, Kim HW, Cheon SY, Lee JE, Kim GW. Apoptosis signal-regulating kinase-1 aggravates ROS-mediated striatal degeneration in 3-nitropropionic acid-infused mice. Biochem Biophys Res Commun 2013;441:280-5.

55. Lee JM, Ivanova EV, Seong IS, Cashorali T, Kohane I, Gusella JF, et al.

Unbiased gene expression analysis implicates the huntingtin polyglutamine tract in extra-mitochondrial energy metabolism. PLoS Genet 2007;3:e135.

56. Solesio ME, Saez-Atienzar S, Jordan J, Galindo MF. 3-Nitropropionic acid induces autophagy by forming mitochondrial permeability transition pores rather than activating the mitochondrial fission pathway. Br J Pharmacol 2013;168:63-75.

57. Strand AD, Baquet ZC, Aragaki AK, Holmans P, Yang L, Cleren C, et al. Expression profiling of Huntington's disease models suggests that brain-derived neurotrophic factor depletion plays a major role in striatal degeneration. J Neurosci 2007;27:11758-68.

58. Benoit ME, Tenner AJ. Complement protein C1q-mediated neuroprotection is correlated with regulation of neuronal gene and microRNA expression. J Neurosci 2011;31:3459-69.

59. Akaike T, Weihe E, Schaefer M, Fu ZF, Zheng YM, Vogel W, et al. Effect of neurotropic virus infection on neuronal and inducible nitric oxide synthase activity in rat brain. J Neurovirol 1995;1:118-25.

60. Goldsmith SK, Wals P, Rozovsky I, Morgan TE, Finch CE. Kainic acid and decorticating lesions stimulate the synthesis of C1q protein in adult rat brain. J Neurochem 1997;68:2046-52.

61. Huang J, Kim LJ, Mealey R, Marsh HC, Jr., Zhang Y, Tenner AJ, et al. Neuronal protection in stroke by an sLex-glycosylated complement inhibitory protein. Science 1999;285:595-9.

62. Fan R, Tenner AJ. Complement C1q expression induced by Abeta in rat hippocampal organotypic slice cultures. Exp Neurol 2004;185:241-53.

63. Ziccardi RJ. Spontaneous activation of the first component of human complement (C1) by an intramolecular autocatalytic mechanism. J

Immunol 1982;128:2500-4.

64. Tenner AJ. Membrane receptors for soluble defense collagens. Curr Opin Immunol 1999;11:34-41.

65. Trouw LA, Blom AM, Gasque P. Role of complement and complement regulators in the removal of apoptotic cells. Mol Immunol 2008;45:1199-207.

66. Taylor PR, Carugati A, Fadok VA, Cook HT, Andrews M, Carroll MC, et al. A hierarchical role for classical pathway complement proteins in the clearance of apoptotic cells in vivo. J Exp Med 2000;192:359-66.

67. Lillis AP, Greenlee MC, Mikhailenko I, Pizzo SV, Tenner AJ, Strickland DK, et al. Murine low-density lipoprotein receptor-related protein 1 (LRP) is required for phagocytosis of targets bearing LRP ligands but is not required for C1q-triggered enhancement of phagocytosis. J Immunol 2008;181:364-73.

68. Farber K, Cheung G, Mitchell D, Wallis R, Weihe E, Schwaeble W, et al. C1q, the recognition subcomponent of the classical pathway of complement, drives microglial activation. J Neurosci Res 2009;87:644-52.

69. Stevens B, Allen NJ, Vazquez LE, Howell GR, Christopherson KS, Nouri N, et al. The classical complement cascade mediates CNS synapse elimination. Cell 2007;131:1164-78.

70. Acevedo-Torres K, Berrios L, Rosario N, Dufault V, Skatchkov S, Eaton MJ, et al. Mitochondrial DNA damage is a hallmark of chemically induced and the R6/2 transgenic model of Huntington's disease. DNA Repair (Amst) 2009;8:126-36.

71. Fernagut PO, Diguet E, Stefanova N, Biran M, Wenning GK, Canioni P, et al. Subacute systemic 3-nitropropionic acid intoxication induces a

distinct motor disorder in adult C57Bl/6 mice: behavioural and histopathological characterisation. Neuroscience 2002;114:1005-17.

72. Brouillet E. The 3-NP Model of Striatal Neurodegeneration. Curr Protoc Neurosci 2014;67:9 48 1-9 14.

73. Brouillet E, Guyot MC, Mittoux V, Altairac S, Conde F, Palfi S, et al. Partial inhibition of brain succinate dehydrogenase by 3-nitropropionic acid is sufficient to initiate striatal degeneration in rat. J Neurochem 1998;70:794-805.

74. Brouillet E, Hantraye P. Effects of chronic MPTP and 3-nitropropionic acid in nonhuman primates. Curr Opin Neurol 1995;8:469-73.

75. Vonsattel JP. Huntington disease models and human neuropathology: similarities and differences. Acta Neuropathol 2008;115:55-69.

76. Colin E, Zala D, Liot G, Rangone H, Borrell-Pages M, Li XJ, et al. Huntingtin phosphorylation acts as a molecular switch for anterograde/retrograde transport in neurons. Embo J 2008;27:2124-34.

77. Zhang J, Peng Q, Li Q, Jahanshad N, Hou Z, Jiang M, et al. Longitudinal characterization of brain atrophy of a Huntington's disease mouse model by automated morphological analyses of magnetic resonance images. Neuroimage 2009.

78. Ermak G, Hench KJ, Chang KT, Sachdev S, Davies KJ. Regulator of calcineurin (RCAN1-1L) is deficient in Huntington disease and protective against mutant huntingtin toxicity in vitro. J Biol Chem 2009.

79. Bachoud-Levi AC, Remy P, Nguyen JP, Brugieres P, Lefaucheur JP, Bourdet C, et al. Motor and cognitive improvements in patients with Huntington's disease after neural transplantation. Lancet 2000;356:1975-9.

80. Fujimura H, Altar CA, Chen R, Nakamura T, Nakahashi T, Kambayashi J, et al. Brain-derived neurotrophic factor is stored in human platelets and released by agonist stimulation. Thromb Haemost 2002;87:728-34.
81. Karege F, Schwald M, Cisse M. Postnatal developmental profile of brain-derived neurotrophic factor in rat brain and platelets. Neurosci Lett 2002;328:261-4.
82. Borrell-Pages M, Canals JM, Cordelieres FP, Parker JA, Pineda JR, Grange G, et al. Cystamine and cysteamine increase brain levels of BDNF in Huntington disease via HSJ1b and transglutaminase. J Clin Invest 2006;116:1410-24.
83. Lim D, Fedrizzi L, Tartari M, Zuccato C, Cattaneo E, Brini M, et al. Calcium homeostasis and mitochondrial dysfunction in striatal neurons of Huntington disease. J Biol Chem 2008;283:5780-9.
84. Zuccato C, Valenza M, Cattaneo E. Molecular mechanisms and potential therapeutical targets in Huntington's disease. Physiol Rev 2010;90:905-81.
85. Luo X, Weber GA, Zheng J, Gendelman HE, Ikezu T. C1q-calreticulin induced oxidative neurotoxicity: relevance for the neuropathogenesis of Alzheimer's disease. J Neuroimmunol 2003;135:62-71.
86. Jung H, Seong HA, Manoharan R, Ha H. Serine-threonine kinase receptor-associated protein inhibits apoptosis signal-regulating kinase 1 function through direct interaction. J Biol Chem 2010;285:54-70.
87. Bialas AR, Stevens B. TGF-beta signaling regulates neuronal C1q expression and developmental synaptic refinement. Nat Neurosci 2013;16:1773-82.
88. Waggoner SN, Cruise MW, Kassel R, Hahn YS. gC1q receptor ligation selectively down-regulates human IL-12 production through activation

of the phosphoinositide 3-kinase pathway. J Immunol 2005;175:4706-14.

< ABSTRACT(IN KOREAN)>

신경손상에 의한 선택적 선조체 병변형성 기작에서의 ASK1의 역할

<지도교수 이 종 은>

연세대학교 대학원 의과학과

조 경 주

본 연구는 유전적 변이와는 관계없이 세포사멸을 유도하는 3-nitropropionic acid 처치에 의한 신경세포 손상기전이 선조체 병변 형성에 국한되는 기전을 ASK1에 의한 조절과 관련하여 살펴보고자 한다. 신경퇴행성질환을 포함하여 뇌의 특정 부위에 국소적 병변이 형성되는 뇌질환은 일반적 병인론과 함께 neuronal loss의 기전 중 하나로서 ubiquitin-proteasome system (UPS)과 autophagy가 보고되고 있다. 내외부적 요인으로 인해 손상된 신경세포는 생존을 위해 비정상 독성 단백복합체에 의해 유발되는 UPS와 autophagy 과정을 처리과정을 시행하고, 최종적으로 dysfunction synapse 의 synapse loss, impaired autophagy 및 apoptosis에 의한 neuronal loss과정을 걷게 된다. 이때 3-NP 주입과

헌팅톤병은 전신적으로 독성물질에 노출됨에도 불구하고 선조체에만 국소적으로 병변이 형성되는 특징이 있다.

이에 본 연구는

(1) 신경독소인 3-NP에 의해 과발현된 ASK1이 이후 하위단계의 변화를 통해 뇌의 부위 (striatum vs cortex)에 따라 서로 다른 세포사멸기작을 유도함으로 3-NP에 의한 감수성 형성에 관여할 것으로 생각되어 대뇌피질 부위와 선조체 부위에서의 세포사멸 기작 및 이에 관여하는 물질 및 분자기전을 살펴보고자 하였으며,

(2) 이를 기반으로 확장된 적용으로서 선조체에 선택적으로 병변이 생기는 헌팅턴병의 경우에서 병의 진행에 따라 증가하는 C1q의 분비량 증가여부 및 그 조절 기작에서의 ASK과의 연관성을 살펴봄으로 선택적 병변형성에서의 ASK1의 역할과 병변형성에 관여하는 새로운 기전을 살펴보고자 하였다.

신경퇴행성질환을 포함하여 뇌의 특정 부위에 국소적 병변이 형성되는 뇌질환은 일반적 병인론과 함께 neuronal loss의 기전 중 하나로서 ubiquitin-proteasome system (UPS)과 autophagy가 보고되고 있다. 세포는 기본적으로 잘못 형성된 단백질을 인지하여 그 변형 단백질을 refold하거나 제거하는 세포간 적절한 네트워크를 통해 건강한 단백질을 유지하고 있다. 이를 수행하는 세포 내 시스템은 chaperon 시스템으로 chaperon은 대부분의 비정상 단백질을 처리할 수 있는 충분한 수용능력을 갖고 있다. 그러나 잠재된 내부적 요인 혹은 외부적인 손상에 의해 생성된 비정상 단백질이 너무 많아 처리 수용 한계를 넘는다면 비정상 단백질 처리 (clearance)를 위한 또 다른 시스템을 가동하게 된다. 내외부적 요인으로 인해 손상된 신경세

포는 생존을 위해 비정상 독성 단백복합체에 의해 유발되는 UPS와 autophagy 과정을 처리과정을 시행하고, 최종적으로 dysfunction synapse 의 synapse loss, impaired autophagy 및 apoptosis에 의한 neuronal loss과정을 걷게 된다. 이때 3-NP 주입과 헌팅톤병은 전신적으로 독성물질에 노출됨에도 불구하고 선조체에만 국소적으로 병변이 형성되는 공통적인 특징이 있다. 이러한 striatal vulnerability는 striatum에서의 특징적인 변화로 야기되는 cell-autonomous mechanism과 striatum이외의 다른 부위에서의 변화에 의해 결과적으로 specific striatal neuronal loss를 가져오는 non-cell-autonomous process로 설명된다. 대표적으로 받아들여지고 있는 설명은 (1) cortex로부터의 BDNF 공급 차단에 의한 striatal neuron의 BDNF 결핍에 의한 striatal degeneration (2) cortex로부터 과분비된 glutamate로 유발된 excitotoxicity에 의한 selective vulnerability로 요약할 수 있다.

Mitogen-Activated Protein Kinase Kinase Kinase (MAPKKK) 신호전달계의 최상위 단계인자이며, 다양한 세포손상에서 주된 조절자 역할을 하는 것으로 보고되고 있는 세포고사신호조절키나아제(Apoptosis signal-regulating kinase 1, ASK1)는 모든 세포에 광범위하게 존재하는 155 혹은 170 kD의 단백질이다. ASK1은 MAPKKK 신호전달계의 최상위 단계인자로서 역할과 더불어 다양한 퇴행성 뇌질환에서의 세포사멸에 관여한다는 보고들이 발표되고 있으나, 현재까지는 세포 내 축적된 퇴행성 물질에 의해 유도된 ER stress의 초기 신호 반응자로서 세포고사 기전에 참여하는 것으로만 발표되고 있다. 그러나, kinase 도메인을 포함한 3개의 도메인을 포함하고

있을 뿐 아니라, 다양한 세포 내 환경에 따라 발현량의 변화를 나타내는 ASK1의 세포의 운명 조절자로서의 역할은 특정 부위의 신경세포에서의 조절 역할에 대해서는 거의 보고 되지 않고 있다. 이에 따라 ASK1의 발현량 조절과 발현량 조절에 따른 분자수준의 변화는 선택적 세포사멸 기전을 이해하는 데 중요한 역할을 할 것으로 예상한다.

한편, innate immune response의 classic pathway의 initiation factor인 C1q의 분비량의 변화 및 이로 인한 microglia activation은 지금까지 중추신경계에서는 발생단계에서의 axon pruning이나, synaptic elimination으로 연구가 국한되었으나, 최근 들어 퇴행성 질환인 알츠하이머병이나, 간질에서 병리기전의 하나로서 연구보고가 되고 있다. C1q의 발현이 neuroprotective effect를 갖는 것으로 보고되고는 있으나, 세포 type별, subregion별, damage 정도에 따라 다르게 작용하고 그 해석도 다양하다. 본 연구는 synapse dysfunction 초기에 증가되는 C1q를 증상이 시작되는 좋은 prediction marker로서의 가능성을 연구하며 ASK1가 매개된 조절 기작 여부를 조사함으로 synaptic loss 또한 보호할 수 있는지 여부를 연구하고자 한다. 그동안 많은 연구자들의 노력으로 신경퇴행성질환의 병인 물질 및 뇌세포 사멸 기작들이 밝혀지고는 있으나, 아직까지 근본적인 치료가 없을 뿐 아니라, 퇴행성 뇌질환의 특징인 뇌의 특정 지역에서만 국한적으로 병변이 형성되어 각 신경퇴행성질환마다 특징적인 행동이상 및 인지기능 이상을 가져오게 되는 선택적 병변형성 기작 및 이에 대한 예측인자의 발굴을 더욱 절실히 요구되는 연구과제라고 할 수 있다.

이를 위한 연구수행 결과, 아래와 같은 결과들을 얻을 수 있었

다. **첫째**, ASK1의 발현억제는 헌팅톤 유발 마우스에서 비정상 헌팅틴 단백질 조각의 핵으로의 이동 및 ER stress 를 감소시켰다. 본 연구를 통하여 헌팅턴 유발 마우스에서 ASK1 단백질의 양과 ER stress는 증가 되어있음을 확인할 수 있었으며, 증가된 ASK1은 비정상 헌팅틴과 결합하여 핵으로의 이동에 영향을 미쳤음을 확인하였다. 결과적으로 ER stress를 유발한다는 것을 보여주었다. **둘째**, 3-nitropropionic acid (3-NP)를 이용한 선조체 병변유발 마우스 모델에서 ASK1은 증가된 활성산소종 (ROS)이 매개하는 선조체 병변을 더욱 악화시킴을 확인하였다. 3-NP 전신주입은 선조체에 선택적 병변을 형성하며, 3-NP의 주된 병변기작인 ROS를 감소시킨 SOD1 유전자변형 마우스에서도 병변을 형성하되 그 크기는 적었다. 과발생한 활성산소종이 많을수록 산화적 손상 및 ASK1의 단백질량과 그 활성도가 병변이 형성된 선조체에서 더 많이 관찰됨을 확인하였다. 본 연구를 통해서는 3-NP에 의해 과발생한 활성산소종이 병변형성에 주된 역할을 하지만, 활성산소종에 의한 이후 반응에 있어서 ASK1이 중요한 역할을 함을 보였다. 활성산소종을 제거하는 효소가 과발현된 SOD1 유전자 변형쥐에 ASK1의 합성한 펩타이드를 주입하면, 동일한 3-NP 주입에도 활성산소종의 양이 증가한 것이 아님에도 불구하고 심하게 병변이 형성됨을 확인하였다. 이것은 ROS의 양을 변화시키지 않더라도 ASK1의 단백질 양이 선조체에서의 신경세포 사멸을 야기할 수 있음을 시사하였다. 그러므로 본 연구의 결과는 신경퇴행성 질환을 포함한 선조체 병변의 치료를 위해 활성산소종의 처치 뿐 아니라 이와 더불어 ASK1의 발현량을 조절함으로 더욱 효과적인 치료가 될 수 있을 것으로 제안할 수 있었다. **셋째**, 3-NP의 전신주입에 의한 선조체 병변형성에 있어서의 ASK1

의 역할이 신경세포에서 뿐만 아니라, 성상세포에서 분비되는 TGF-beta를 조절하고, 성상세포에서 분비된 TGF-beta는 신경세포에서의 선천면역의 complement factor중의 하나인 C1q의 발현 및 분비량을 조절함으로 선조체 병변형성을 위한 기전에 중요한 역할을 하는 것을 확인하였다. 3-NP 전신주입에 의한 미토콘드리아 기능이상은 세포 내 활성산소종을 과발현시켰고, 선조체에서의 BDN혈를 고갈시켰다. 그런데, 3-NP의 전신주입에 의해 선조체에서 선택적으로 일어나는 변화 중 성상세포가 선조체 측면에서 강하서 활성화 되는 것을 확인하였며, 이때 TGF-beta의 유전자 수준이 선조체 부위의 세포에서 크게 증가할 뿐 아니라, 이와 상응하여 혈액에서의 TGF-beta의 분비량이 증가함을 확인하였다. 이와 더불어 TGF-beta에 의해 조절 받는다고 보고된 바 있는 C1q의 유전자 발현 정도와 혈액에서의 분비량 모두 TGF-beta에 상응하여 변화되는 것을 확인 할 수 있었다. 이에 ASK1은 성상세포의 TGF-beta의 조절과 연관되어 있으며, 이에 의한 신경세포에서의 C1q 분비 정도를 변화시킬 수 있은 것으로 확인되었다. 이것은 대뇌의 특정부위에 병변이 형성되는 신경퇴행성 질환 및 3-NP에 의한 선조체 병변 형성에 면역인자가 관여되는 또 하나의 가능성 있는 기전을 제공할 뿐만 아니라, 유전자변이를 갖고 태어난 헌팅턴병 환자들의 경우, C1q의 혈액내로의 분비량의 변화를 측정함으로 병증의 증상개시 시기를 예측할 수 있는 표지인자로서의 사용 가능성 또한 제시할 수 있을 것으로 생각된다.

핵심되는 말: 세포고사신호조절 키나아제, 헌팅톤병, 3-nitropropionic acid, brain derived neurotrophic factor, siRNA, superoxide dismutase

PUBLICATION LIST

1. **Cho KJ**, Kim HW, Cheon SY, Lee JE, Kim GW. Apoptosis signal-regulating kinase-1 aggravates ROS-mediated striatal degeneration in 3-nitropropionic acid-infused mice. Biochemical and biophysical research communications. 2013;441(2):280-5.

2. Song J, **Cho KJ,** Cheon SY, Kim SH, Park KA, Lee WT, et al. Apoptosis signal-regulating kinase 1 (ASK1) is linked to neural stem cell differentiation after ischemic brain injury. Experimental & molecular medicine. 2013;45:e69.

3. Kim HW, **Cho KJ,** Lee SK, Kim GW. Apoptosis signal-regulating kinase 1 (Ask1) targeted small interfering RNA on ischemic neuronal cell death. Brain research. 2011;1412:73-8.

4. **Cho KJ**, Lee BI, Cheon SY, Kim HW, Kim HJ, Kim GW. Inhibition of apoptosis signal-regulating kinase 1 reduces endoplasmic reticulum stress and nuclear huntingtin fragments in a mouse model of Huntington disease. Neuroscience. 2009;163(4):1128-34.

5. Minn Y, **Cho KJ,** Kim HW, Kim HJ, Suk SH, Lee BI, et al. Induction of apoptosis signal-regulating kinase 1 and oxidative stress mediate age-dependent vulnerability to 3-nitropropionic acid in the mouse striatum. Neuroscience letters. 2008;430(2):142-6.